The Effects of Altering Air Velocities in Operational Clean Rooms

by

Maribel Vázquez

B.S., Mechanical Engineering
Cornell University, 1992

Submitted to the Department of Mechanical Engineering
in Partial Fulfillment of the Requirements for the Degree of
Master of Science in Mechanical Engineering

at the

Massachusetts Institute of Technology

June 1996

Signature of Author.....
Department of Mechanical Engineering
May 10, 1996

Certified by.....
Leon R. Glicksman
Professor of Architecture and Mechanical Engineering
Thesis Supervisor

Accepted by.....
Ain A. Sonin
Professor of Mechanical Engineering
Chairman, Department Committee on Graduate Students

Acknowledgments

I would like to thank some very special people who contributed to the development of this research and thesis. First, I thank Ruben Rathnasingham for introducing me to the wonders of spot welding hot wire anemometers. Second, I wholeheartedly thank Wesley McDermott, for designing the electrical circuit which made data collection possible. Special thanks to my wonderful advisor, Leon Glicksman, for his support and words of encouragement throughout this entire research, and I would like to thank Paul McGrath, from Microsystems Technology Laboratory, for his tremendous help during setup and experiments. Additionally, this author thanks the National Consortium for Graduate Degrees for Minorities in Engineering and Science, Inc. (GEM) whose funding made graduate study possible. Lastly, I wish to especially thank Carl Loeffler who provided continued laughter and support during the experiments and writing of this thesis.

Especialmente dedicado a Ilialis Hernandez, quien siempre tuvo fe en mi.

The Effects of Altering Air Velocities in Operational Clean Rooms

by

Maribel Vázquez

Submitted to the Department of Mechanical Engineering
on May 10, 1996 in partial fulfillment of the
requirements for the Degree of Master of Science in
Mechanical Engineering

Abstract

Experimental studies measuring velocity profiles, particle deposition and energy consumption were performed in an operational class 10 clean room. The research utilizes constant temperature hot wire anemometers to gather velocity profiles and analyze turbulence intensities for 50 feet per minute(FPM), 70FPM, and 90FPM air velocities. To measure particle deposition rates, particles were injected and retrieved with the use of test wafers and a wafer inspection station.

The results indicate higher air velocities increase particle deposition. Additionally, the velocity profiles indicate a homogeneously turbulent flow midway from the air source to exhaust path. However, turbulence intensities do demonstrate the dissipation of air unidirectionality close to the floor. Subsequent particle counts indicate operational clean rooms may reduce their air velocities and remain within their current class level. The research suggests a reduction from 110FPM to 50FPM will save a modern facility $320,000 a year in operational costs and simultaneously maintain low particle counts.

Thesis Supervisor: Leon R. Glicksman

Title: Professor of Architecture and Mechanical Engineering

Table of Contents

List of Figures and Tables

Chapter 1

1.1- Introduction

The semiconductor and microelectronics industries have produced a wide variety of modern products including microwaves, calculators, pagers, mobile phones, stereos, automobiles, keyboards, and computers. However, these multibillion dollar industries, among others, are themselves dependent upon clean rooms whose controlled environments enable the manufacturing process. The electronics needed in today's home appliances require a clean room environment to eliminate dust or dirt from the product; clean rooms filter particulates from the incoming air which may cause product failure or malfunction. By providing such environments, clean rooms have enabled the manufacture of the numerous microelectronics and semiconductors so prevalent in the modern world.

Unfortunately, high quality clean room facilities have been limited to large scale corporate users because of the time and cost associated with their design and construction. With a minimum of 6 months for design and 12 months for construction, the cost of a fully sized clean room facility ranges between $200 million and $300 million dollars. Since a facility generally holds only 64,000 square feet of clean space, the true cost of clean rooms ranges between $3100 and $4700 per square foot. Shockingly, this estimate reflects solely the cost of the edifice; the required process tools and their installation may in some cases triple the total cost. These exorbitant costs are forcing smaller users to embark upon joint ventures, sharing clean rooms, and often product designs, with their competitors. [1] In addition, since the first product on the market has traditionally enjoyed over 75% of the after market profits, clean room costs

are driving larger users to build facilities faster and faster in an attempt to produce the first marketed product.

Since clean rooms are designed to support a manufacturing process, the facility is classified in response to the process needs. As a result, clean room environments require large supporting facilities, and energy consumption becomes a weighty obstacle during operation. Over 10,000 gallons of domestic water are used monthly in a typical clean room facility, producing a near equal amount of effluent. Typical electrical costs range from $24,000 to $35,000 a month, and the comprehensive cost(water, electricity, effluent etc..) of 1 cubic foot of air exhaust is approximately $25 per year. Since clean rooms operate 24 hours a day, 7 days a week, year round, these costs compound to reach an exorbitant amount very quickly. However, because the past two decades have been ones of amazing growth for the clean room industry, many researchers have failed to take a step backwards and reanalyze why clean room facilities have grown so large, and their costs so phenomenal.

Part of the issue is that antiquated operating specifications are still currently employed. The industry has foolhardily relied upon the original clean room model, developed decades ago, to provide the optimal parameters for today's facilities. The resulting overestimated specifications drive enormous facility systems and subsequent operating costs. Because so few researchers have reexamined the clean room industry from an operational standpoint, clean rooms have been condemned to a life of energy inefficiency. However, the present research will identify new methods to lower clean room energy consumption by analyzing the air handling systems and air velocity specifications. The major goal will be to study the correlation between velocity profiles

and particle deposition rates in order to examine how lowering air velocities will increase clean room energy efficiency and performance.

Chapter 2

2.1 History

Clean rooms produce the manufacturing environment for highly sophisticated designs as well as the familiar home devices. Perhaps the first serious users of the clean room were the United States military and the aerospace industry. During World War I, controlled environments were built to eliminate the gross contamination associated with the manufacturing areas for aircraft instruments. Heavy dust-laden air was a frequent cause of failure in small bearings and gears used in the first aircraft instruments. In attempting to control the area's level of contamination, the military became the first to create what was essentially a clean room. Shortly thereafter, the aerospace industry used the clean room concept when first exploring the idea of satellites; miniature satellite components were assembled in contamination-free environments in order to prevent equipment failure during orbit. Clean room technology proved so valuable for the aerospace industry, that clean rooms are still used extensively today in the testing of space vehicles and in the assembly of their instrumentation.

As clean room technology evolved, it become integral in many other industries as well. For instance, the nuclear industry currently utilizes clean rooms for the segregation of radioactive materials, production of fuel rods, and assembly of radioactive devices. The pharmaceutical industry recently began incorporating contamination free manufacturing in the production of pharmaceuticals and biological materials. In the medical profession, the amazing evolution of the operating room has merited the designation of its own clean room class. This designation seems obvious

since the very definite need for environment control in these rooms is evident from the meticulous care the surgeons and medical staff must undertake during "scrub-up" procedures. Other less commonly known users of clean rooms are telecommunications companies for cable shielding, the food processing industry for synthetic production and packaging, and even the skiing industry for its use of fiberglass. Among the largest users of the modern day clean room is the semi-conductor industry. Because of the contamination related problems inherent in semi-conducting processing, microelectronics that are now commonplace would be inconceivable without the development of clean rooms. Modern circuitry is often so minute, that it may be destroyed by a particle one one-hundredth the diameter of a human hair as illustrated in Figure 2.1.

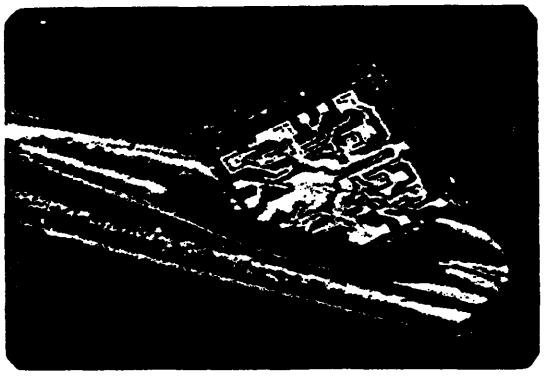

FIGURE 4-5. Passing a circuit through the eye of a needle.

Figure 2.1 - Microelectronics

2.2 Particles

The underlying theory of clean rooms is a fairly straightforward one: A clean room is a room in which efforts have been made to control the amount of particulate

matter within it. However, the degrees of effort and quantity of particulate matter define the type of clean room; a typical facility can only sustain a clean environment with less than 1000 particles per 100 cubic foot. Particulate matter is any particle present in a flow stream. Particles may be found in gasses, liquids and solids, as either suspended or settled materials. Particulate matter which appears in all geometries and configurations, and can be organic or inorganic, often has microscopic dimensions. Virtually all tangible objects emit particles. Paper, pens, wood, clothes, and humans all emit them. People emit extremely large quantities of particulates when performing even minimal activity. For instance, humans emit 100,000 particles per minute merely when standing still. Table 2.1 illustrates the quantity of particles emitted by simple activities:

Light head and arm motions	500,000 Particles per minute
Average arm motions	1,000,000 Particles per minute
Standing up from a sitting position	2,500,000 Particles per minute
Slow walk(2mph)	5,000,000 Particles per minute
Climbing stairs	10,000,000 Particles per minute
Running	30,000,000 Particles per minute * Particles of 0.5 micron diameter or larger

Table 2.1 - Human Particle Emission Data

These particles are predominantly emitted from human skin and hair, which consist of salt microcrystals and the protein Keratin, respectively. The skin particulates range between 0.1 micron to 5.0 microns in diameter, while the diameters of hair particulates

range between 5.0 microns and 100 microns. Since the goal of a clean room is to eliminate particles entirely, Table 1 indicates that clean rooms can not tolerate normal human activity. Hence, due to the unacceptable amount of particles produced by continued human activity, clean room personnel are required to wear specific clean room attire, often referred to as "bunny suits". These overgarments are usually made of Gortex and cover the arms, legs, hands, feet and head of an operator. The eyes are protected with laboratory goggles, but the cheeks and nose are left unprotected to facilitate breathing. However, as effective as these overgarments are, they still cannot eliminate particle generation entirely and as a result, various other engineering solutions are implemented in clean room particulate removal.

2.3 Air Filtration

The clean room industry considers a specific material a contaminant if it meets two criteria: the particle must have the physical properties to cause damage and the means to migrate to a vulnerable location. Salt and Keratin, in particular, can generate sufficient ionic effects on semi-conductor wafers to cause extensive damage. However, a particle's ability to migrate to vulnerable locations is dependent upon clean room filtration and airflow. Hence, the control of airborne and transfer particles becomes the central function of any clean room.

For the control of airborne and transfer particulates, clean rooms utilize High Efficiency Particulate Air filters commonly known as HEPA filters. These specialized filters remove 99.9997% of particles less than 3.0 microns in diameter from the air. These types of filters were first developed by the Chemical Warfare Service(CWS) for

the improvement of gas masks during World War II. Later, during the development of the first atomic bomb, the Manhattan Project utilized the CWS filter to capture radioactive dust in order to prevent lethal radioactive doses. The scientists then perfected the filter and was the first organization to use them for area filtration. [2]

Although the numerous mechanisms enabling HEPAs to achieve high filtration levels are complex, their construction is straightforward. Very fine glass fiber filaments, with diameters ranging from a millimeter to less than a fraction thereof, are formed onto a thin pad and held into place by a resin bonding agent. The pad has an open structure such that the interstices are no less than 100 micrometers wide and allow air passage with a relatively low pressure drop(.3"-.5" of water typical). The glass fiber pad is then folded around corrugated separations enabling a larger airflow with a larger filter surface area. HEPA construction is illustrated in Figure 2.2.

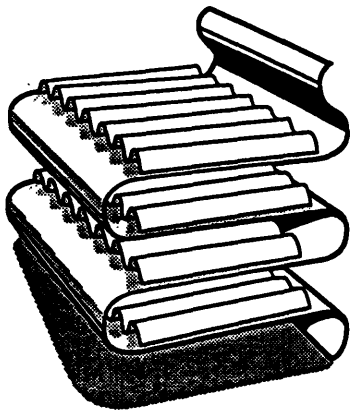

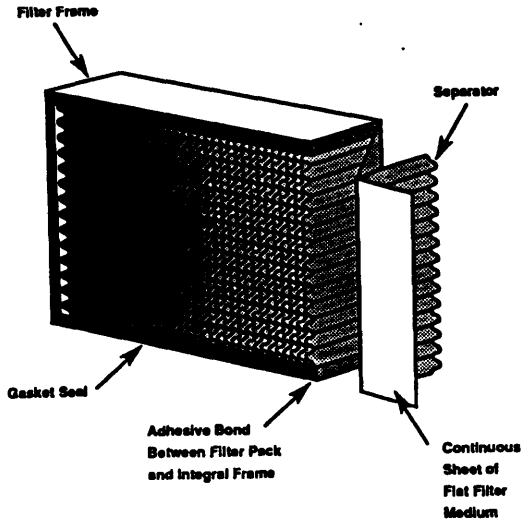

Figure 4-4 HEPA filter construction.

Figure 2.2- HEPA Construction

The three mechanisms of filtration are interception, impaction, and diffusion. The filter interstices capture particles with diameters greater than 5 microns through interception because the particles' "large" size prevents passage through the filter structure. Medium sized particles with diameters greater than 0.5 microns are often caught by impaction as they collide with the filter fibers while traveling through the filter mesh. The smaller particles with diameters less than 0.1 microns will consistently follow the air stream and can only be collected by Brownian diffusion: random air movement displaces the particles until they make contact with filter fibers and adhere to them. Particle adhesion may be attributed to surface chemistry, Van der Waals forces, electrostatic charges or a combination thereof.[3]

2.4 Vertical Laminar Flow

To develop a clean room environment, it is insufficient to merely introduce filtered air into an intrinsically clean area because airflow patterns strongly determine the cleanliness level of a room. In fact, if clean room engineers did not insure a certain type of airflow, there would be little discernible difference between clean rooms and office spaces. Office workers receive filtrated air, albeit not HEPA filtered, upon entering an office building but cannot say they work in clean rooms. The typical office Heating, Ventilation, and Air Conditioning(HVAC) system functions to create good air mixing in the space by introducing filtered air via ceiling grids on one end, and removing well mixed air from the opposite end. The result is a well mixed environment where temperature, odors and particulates are uniformly distributed. The result would be

unsuccessful as a clean room because of the particulate density and distribution. This flow pattern displaces particles in obscure places and reintroduces them into the environment at random locations. Because of this random displacement and uniform mixing, air in the space would not be clean regardless of the degree of filtration.

Ironically, early clean room design was unfortunately closer to this office style system than the current design. These older designs, called Conventional Clean Rooms, introduced filtered air through a fixed number of ceiling grids and extracted air through wall mounted return grilles. As shown in Figure 2.3, the nature of this design generated irregular airflow which was plagued with turbulent eddies, stagnant air zones and dust traps in areas far away from return grilles.

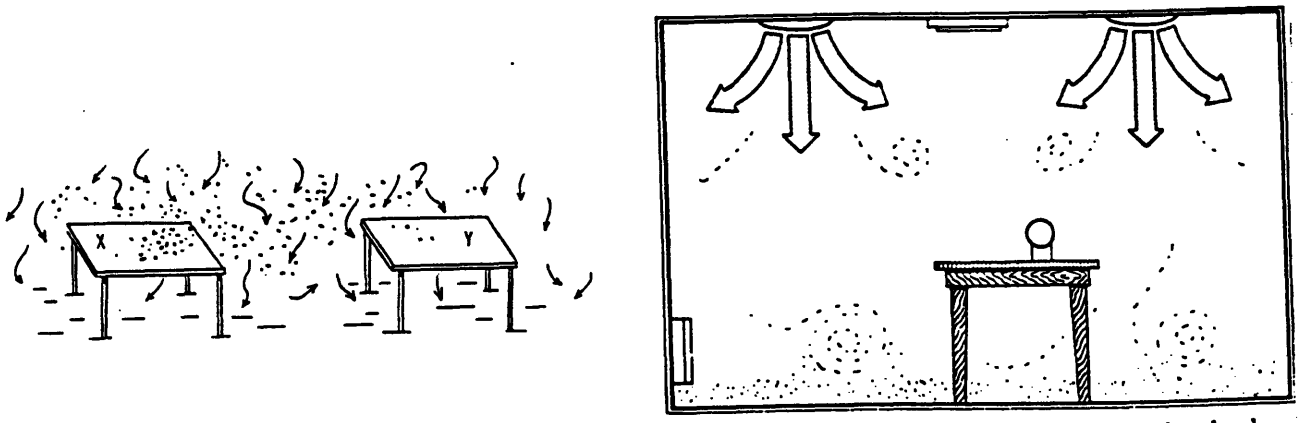

FIGURE - . Air-flow patterns in conventional clean rooms. *Courtesy Sandia Corp.*

Figure 2.3- Conventional Clean Room

Subsequent air studies in these rooms found clear streamlines from ceiling grilles to return grilles, but a large degree of random mixing elsewhere. Obstructions and internal

movements in the air path often displaced air streams to areas far away from return grilles. As a result, cleanliness levels were determined by the time of day and amount of workers in the area instead of by the process. In an attempt to enhance the particulate removal of these rooms, engineers increased air velocities anticipating a greater purging effect. However, the increased air streams resulted in air blasting problems as stray particles on tabletops or operator coveralls were blasted from their original locations to elsewhere in the room. In addition, the faster air streams were susceptible to turbulent eddies far away from return grilles, which embedded particles indefinitely in air stagnant zones. Particle counts later confirmed that larger air velocities in conventional clean rooms contributed to increased particle retention and did not enhance the environment.

Because conventional clean rooms lacked the desired contamination control specifications, subsequent research in the 1960's led to the development of a new clean room airflow pattern, called Vertical Laminar Flow(VLF). Researchers agreed that the crucial design consideration was a greater self-cleaning capability. It appeared that a larger airflow would be a partial solution, however, higher air flows in conventional clean rooms were directly correlated with higher particle counts and air blast issues. The increase in velocity would enhance particulate purging to a point, after which an increased velocity would only stir up more dust and re-introduce it into the room. The solution was to increase the air velocity, but introduce the air through a very large area of diffusers. To maximize available ceiling space and simultaneously minimize velocity, VLF utilized the entire clean room ceiling as a diffuser. HEPAs were placed in every square inch of ceiling space and protected by grilled meshes underneath them. In this

manner large volumes of air could be introduced uniformly throughout the clean room and their flow rate easily adjusted.

Similarly, VLF requires a large enough outlet to enable the large air volumes to flush particles out of the clean room. This was accomplished by replacing the floor with grated floor tiles serving as return grilles. The researchers concluded: "Laminar flow would be produced when air was introduced into a room at a low velocity, into a space confined on 4 sides, through an opening equal to the cross sectional area of the confined space."[4] As seen in Figure 2.4, the result was unidirectional air flow with vertically stratified air streams to insure minimal cross contamination and little or no transfer of energy, and particles, from one streamline to another.

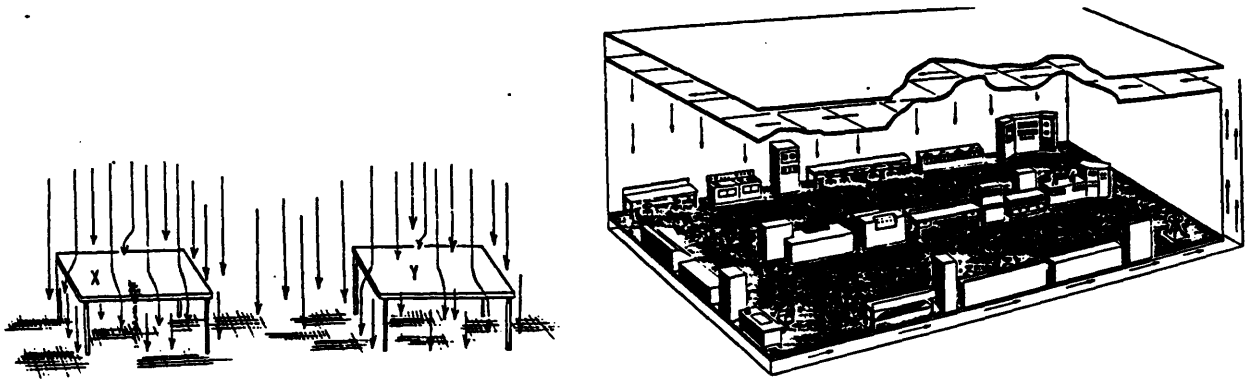

FIGURE - . Equipment layout in down-flow clean room. *Courtesy MAMES, Olmsted AFB, Pa.*

Figure 2.4- Laminar Flow Clean Room

When the VLF prototype clean rooms displayed dramatically lower particle counts than their conventional counterparts, Vertical Laminar Flow was fully adopted into future clean room design.

2.5 Clean Room Configuration

VLF research also includes a new internal clean room configuration to control particle and gas dispersion by physical separation. The main body of a clean room is configured into areas designated as bays and chases with separate airflows. A bay is the area hosting a manufacturing process while its adjacent space facilitating equipment access is called a chase. VLF utilizes this configuration by introducing clean air through the bays and extracting air through the chases. This configuration maintains downward airflow flushing in the areas which sustain direct wafer contact, and upward cleansing in the areas servicing equipment. This configuration is called Reverse Flow and is widely implemented in larger facilities.

2.6 Supporting Facility

Although the size of a clean room facility is measured by its square footage of clean space, the additional facility required to support the clean room environment is quite extensive and its cost exorbitant. Not only does each process require different purity systems and specialized materials, but the conditioning of clean room air demands highly effective, reliable and expensive equipment. The complexity of a clean room facility is illustrated in Figure 2.5:

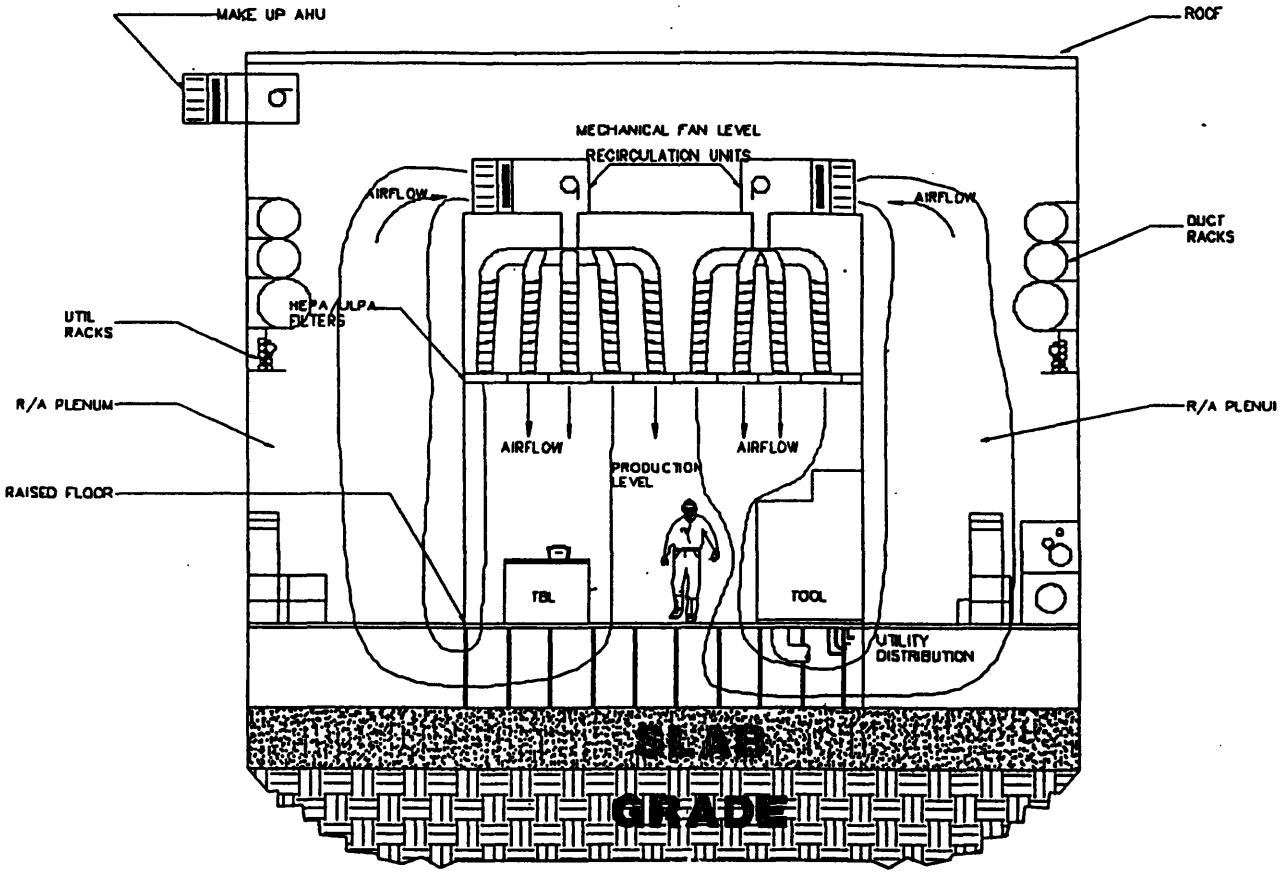

Figure 2.5- Schematic of Typical Clean Room Facility

To maintain air unidirectionality and simultaneously flush out particles, clean rooms circulate over 900,000 cubic feet per minute of clean air. Air filtration and delivery, albeit the most important, is one of the largest and most expensive systems, in any clean room facility. As shown in Figure 2.6, during initial construction the air handling system alone is 18% of the cost.[5]

Figure 2.6- Construction Costs of a Clean Room Facility

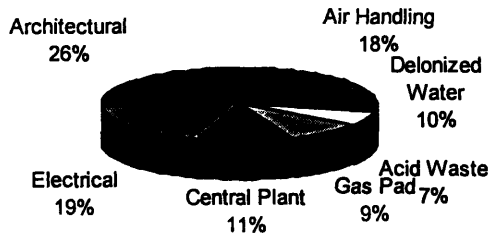

The operating costs of modern clean room facilities range between $30,000 and $40,000 a month for electrical, domestic water, and effluent. A typical air handling system uses $9,000-$12,000 a month of electricity, $3,000 a month for water, and $2,700 a month for effluent.

Air must be extracted from the atmosphere, finely purified, delivered uniformly into the clean room, and then recirculated or exhausted. Special air handling equipment is therefore required to accomplish this crucial clean room task. Two primary types of air handling systems develop the clean room environment: Make Up Air Handlers(MUA), and Recirculating Air Handlers(RAH). Both air handlers work in similar manners with a difference in air purity levels. MUAs constantly extract outside air and condition it downstream. They provide 100% filtered air to the RAHs which combine clean room return air with a percentage of make up air before recirculating it in back into the clean room. A clean room facility generally uses a minimum of 25% make up air and 75% recirculated air.

As shown in Figure 2.7, a Makeup Air Unit(MUA) is an assembly of components that conditions makeup air introduced for both ventilation and replacement of exhausted air. MUAs condition replacement air to match the existing air by heating, cooling, humidifying/dehumidifying, and filtering incoming air. Air handling units accomplish this conditioning through various interacting equipment such as pre-filters, heat exchangers, de/humidifiers, and fans.

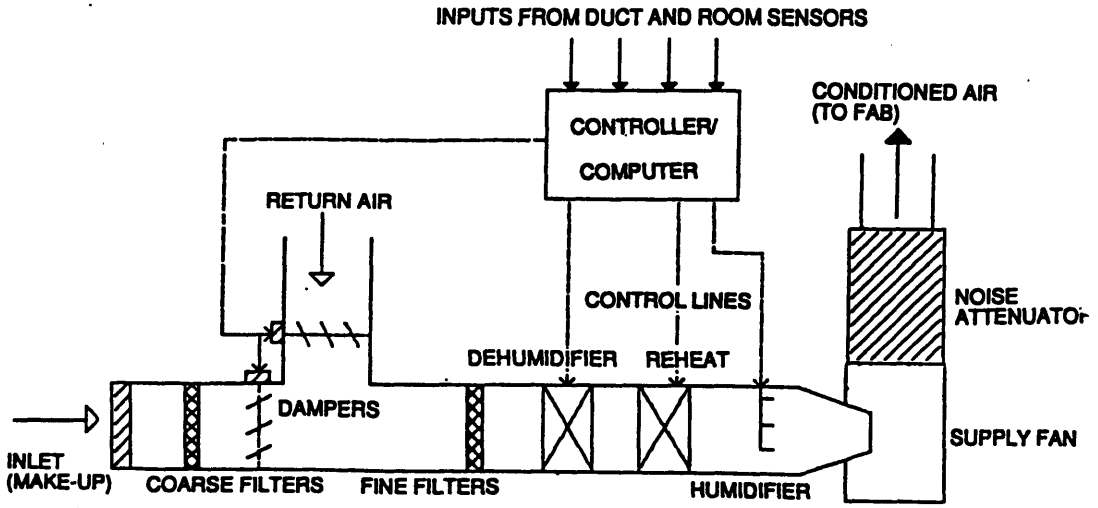

Figure Simple air handler configuration.

Figure 2.7- Air Handling Unit

The air handling process begins with the intake of outside air through louvers. Air handler units generally rest on the roof of a facility for maximum air intake. Louvers are also utilized for their practicality, because their sharp angle prevents large airborne objects from flowing into the remaining air handling system. Air is first extracted from the atmosphere and forced through a series of pre-filters. The first pre-filter is a coarse first pass filter which removes large particles down to 200 micron diameters from the air

stream. The remaining pre-filters are a series of fine 80 micron bag filters which remove medium sized particles (down to 5 microns in diameter) from the entering air stream. Only after the outside air is depleted of these particles is it ready to be introduced through HEPAs. (Since HEPAs are approximately $120 each, it is important not to overload them with air streams containing particles larger than 5 microns.)

After exiting the pre-filters, the refined air travels through a preheat coil for temperature conditioning. This first heat exchanger moderately adjusts the incoming air such that equipment further downstream will not experience extreme temperatures. Upon exiting the preheat coil, the air travels through an air-water coil cooled by chilled water for increased temperature conditioning and perhaps dehumidification. Dehumidification is needed in climates of high humidity whereas humidifiers are used in low humidity regions. Dehumidification is often accomplished through cooling coils because when moist air is cooled, it loses some of its water content through condensation. The limit of its water capacity depends on the air temperature; the higher the temperature the higher the humidity. If air at a particular temperature is saturated with water vapor, a temperature reduction will reduce its water capacity forcing excess water to condense into droplets. Unfortunately, because the amount of water removed increases with decreasing temperature, a reheat coil is often needed to reheat the air after it has been dehumidified. Alternative chemical dehumidification processes are currently available, but are relatively expensive. The alternative replaces the use of cooling coils with desiccants. Desiccants are extremely hydrophilic materials which absorb water from air on contact. The disadvantage of this method is that after a short time desiccants may become saturated with water and no longer absorb water at the

same rate. Desiccants must then be regenerated through heating to drive off absorbed water. During that time humidity control is established through the mixing of dried air from a dehumidifier with moist air from the inlet. The double cost associated with this process is seldom worth the expense. Hence, the dehumidification process is often expensive and energy inefficient, which combined with lower labor and property costs, persuades many users to construct clean room facilities in the friendlier environment of the South West.

The opposite process of humidification is often 100 times less expensive than dehumidification, making it the more energy and cost efficient alternative. One of the most popular methods of humidification is by steam spray, which is particularly ideal for large airflows and volumes since steam sprays can supply 1700 liters an hour of moisture into the air with only 2 pounds per square inch of pressure drop. The drawback of using this method in clean rooms is the requirement of semi-pure spray. If the steam spray contains any contaminants, they will be extremely well dispersed into the subsequent air stream and very difficult to remove. The solution is to use some form of filtered water to create the spray. However, since the water must flow through facility piping, an extremely corrosive fluid will cause extensive damage. Fortunately, clean room facilities utilize several thousands of gallons of semi-pure water each month, which is then recycled and used in the humidification process. However, the use of even this semi-corrosive fluid requires a protective glass liner for the boiler as well as high quality stainless steel piping. Hence, although the overall cost of humidification is much lower than that of dehumidification, it is still far from economical.

Lastly, one of the most important aspects of any air handling unit is its supply fans. A fan is an air pump that creates a difference in pressure and is used to provide a continuous air flow into the clean room facility.[6] Fans produce pressure and/or flow because their rotating impeller blades impart kinetic energy to the air by changing its velocity. In a centrifugal fan, air enters axially then turns at right angles through the blades and is discharged radially. The major advantages of this type of fan are its ability to produce high pressures at relatively low speed and its external motor. With motors located outside of the air duct, centrifugal fans have a definite advantage in the clean room industry because motors introduce an infinite possibility of contaminants from bearings and coils. However, since their large size often becomes a disadvantage, centrifugal fans may often be less desirable than axial flow fans. Axial flow fans receive and exhaust air axially. The fans' motor and blades are placed in the air stream but develop less pressure than their centrifugal counterparts. However, in a large clean room facility where up to five fans may be needed to drive air into a particular area, their compact nature makes axial flow fans the fan of choice in clean room facilities.

2.7 Certification

With such extensive and costly facilities, engineers must take measures to insure their systems are providing the desired clean room environment. Once a clean room is designed, constructed, built and ready for use, the engineers must certify the clean room ready for operation. Certification is the equivalent of calibrating a sophisticatedly designed instrument; it is essential initially as well as periodically throughout the clean room's duration. However, many clean room users do not certify their facilities as

precisely or as often as they should because the cost approaches several hundred thousand dollars.

Certification verifies a facility is operating to the desired specifications by testing all clean room parameters. Certification involves over 12 tests including those designed to verify airflow parallelism, turbulence levels, and air uniformity. Stable vertical streamlines should produce close to zero cross flow. Bays and chases must receive uniform airflow, and velocity fluctuations resulting in turbulent eddies must be avoided. Since eddies embed particles within them rather than flushing them out of the clean room, the turbulence test is designed to single out these currents as they form due to increased air velocity or equipment location. Certification also measures: pressurization, temperature, relative humidity, vibration and sound level, electromagnetic Interference(EMI) and conductivity.

Certification will also "rate" a clean room by determining its class level. Clean rooms have traditionally been rated from Class 10,000 to Class 1 as defined by Federal Standard 209E. Figure 2.8 illustrates the limits on each class. A class 1000 clean room, for instance, indicates the clean space has less than 1000 particles of 0.5 micron diameter or larger within 100 cubic feet. A class 100 clean room indicates there are less than 100 particles within 100 cubic feet. Additionally, the current manufacture of smaller and smaller electrical devices has prompted the new designation of Class Sub 1. This rating certifies the facility has less than a fraction of one particle within 100 cubic feet. A Class Sub 1 designation is extremely prestigious as less than a handful of all semi-conductor clean rooms in the United States conform to these stringent specifications.

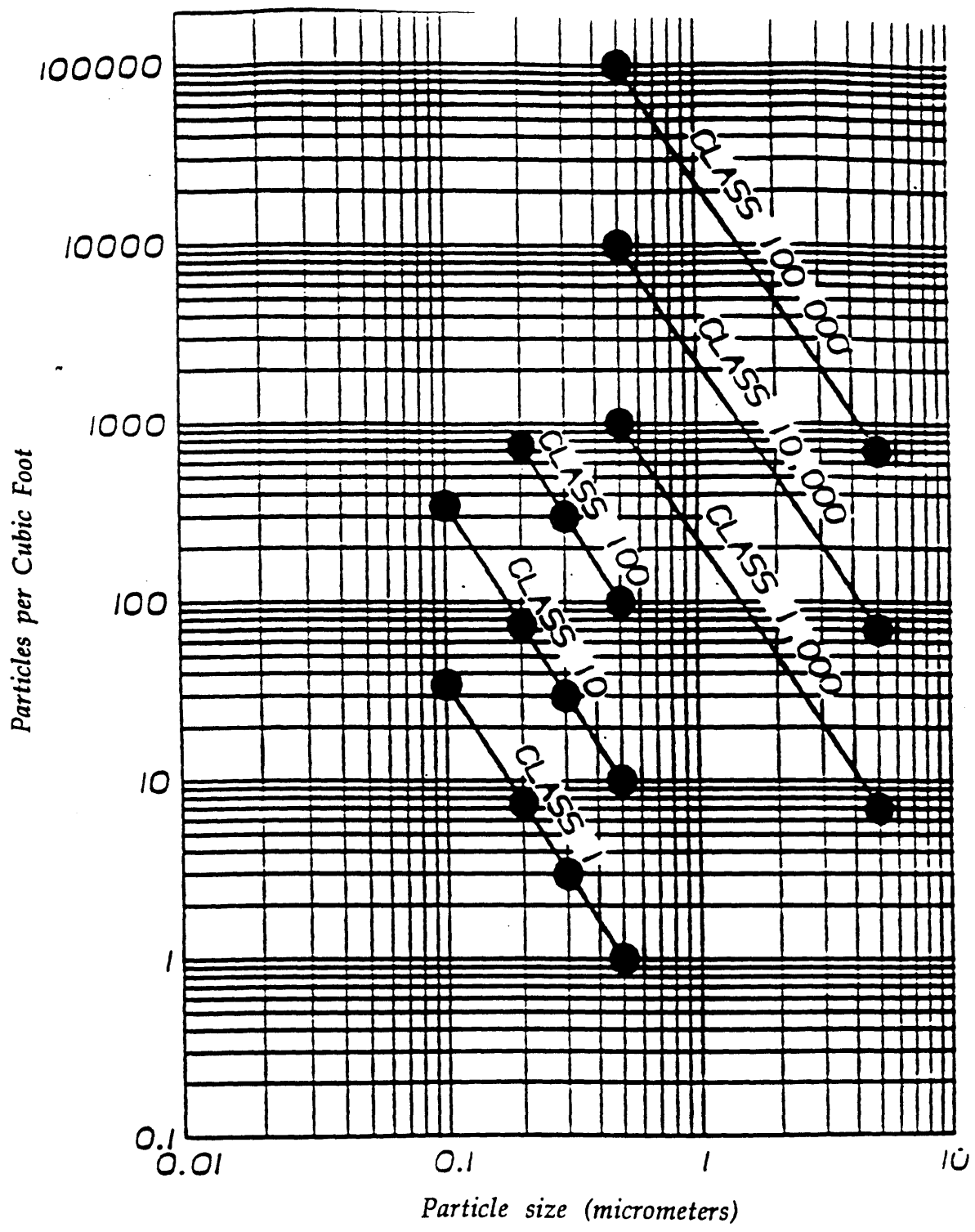

Figure 2.8- Certification Levels for Clean Room Facilities

Chapter 3

3.1 The Laminar Misnomer

This research will not treat clean room airflows as laminar. Clean room air velocities combined with room height yield Reynolds numbers on the order of 10^5. Since air flows with such Reynolds numbers certainly lie in the turbulent regime, they inherently possess an entirely different variety of properties, which makes the convenient assumptions and simplifications of laminar flow inapplicable to flow in clean rooms.

Fluid turbulence in itself is a highly complex phenomenon. Turbulence may be defined as a three dimensional, time dependent motion whose average properties may be independent of position in the fluid. In turbulent flow there are fluctuating velocities in three dimensions even if the mean velocity has only one or two components. In the past, many scientists have also used the term "random" motion to describe turbulence. In this instance, "random" does not imply that an instantaneous velocity becomes independent of the next, but rather indicates that velocities at two points become less closely related with increasing separation. [7]

3.1.1 Velocity Fluctuations

Although there are several defining characteristics of turbulence, this research will analyze only three: velocity fluctuations, self preservation, and spectral analysis. Time varying velocity fluctuations are a defining characteristic of turbulent flow distinguishing it from laminar flow. As shown in Figure 3.1, whereas laminar flows

sustain a steady mean value with little variation, most turbulent flows sustain fluctuations between 0.1% and 10% of the flow's mean value:

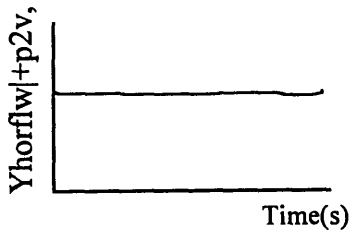

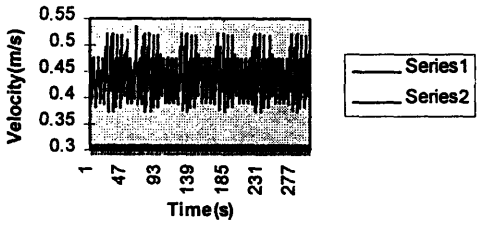

Laminar Flow

Turbulent Flow

Figure 3.1

Not only do turbulent fluctuations vary in magnitude, but also with direction and time. In fact, fluid turbulence develops from the growth of instabilities that lead to this chaotic state. Due to the fluctuations in velocity, the fluid mixes rapidly and momentum is transported quickly. The transverse velocity gradient creates high levels of shear that generate large eddies. The larger eddies will produce smaller and smaller eddies through inertial interaction, and in so doing, transfer energy to them. In this manner, the eddies follow an energy cascade until the kinetic energy is dissipated through viscous friction at the smallest eddy[8]. These velocity fluctuations make it advantageous for the researcher to adopt a new definition of velocity separating velocity into U_o, the mean velocity, and U', its fluctuation:

$$U = U_o + U'. \qquad \_(1)\_$$

The separation of velocity into these components permits an analysis of the fluctuation as a function of the mean. This calculation is called the turbulence intensity and it

provides a means to measure the level of decay in a flow field. Turbulence intensity is defined as the root mean square of the fluctuation divided by the mean flow. The rate of decay in a turbulent flow is critical in turbulent analysis because it provides the spatial range in which turbulent assumptions are valid.

3.1.2 Self Preservation

Turbulent flow fields have the additional distinctive characteristic of self-preservation. In 1940, Karman introduced the characteristic of self-preservation in turbulent flow fields. The term "self-preserving" means that a turbulent flow pattern retains the shape of its velocity function during decay. One indicator of self preservation is the ability to reduce averaged flow properties by characteristic scales that depend on a single variable. For example, if the mean velocity is given by U= U(x,y) then self preservation may imply that there exists a length scale $\delta(x)$ and a velocity scale $U_s(x)$ such that:

$$U = Us \bullet f\left(\frac{y}{\delta}\right) \qquad \_(2)\_$$

An important consequence of this definition is that the equations of motion are reduced by one dimension and as a result, this type of self preservation is most commonly used in boundary layer theory. However, it is the second indicator of self-preservation, called local similarity, which will be used in this research. The principal difference between the two indicators is that local similarity does not lead to a reduction in the order of governing equations. The best application is Kolmogorov's similarity of small scale turbulent motions in high Reynolds number flows. Since clean room airflows are high

Reynolds number flows with small scale fluctuations, this research will utilize the Kolmogorov microscale to identify key parameters for an accurate turbulence model.

Kolmogorov developed the theory that links the decay of large eddies into smaller eddies and dissipation in terms of a power input per unit mass variable. This theory suggests that small scale components of turbulence are approximately in statistical equilibrium. In this hypothesis, turbulent motion is represented as a superposition of periodic eddies with different lengths, time scales, and oscillations in space. The process of energy transmission between the various scales of motion can now be described in terms of interaction between these eddies. Kolmogorov generated the turbulent microscale by studying the dynamics of eddies in the smallest possible scale. He defined the time required for an eddy to dissipate into itself as the viscous time parameter, T_v, and the time required for an eddy to travel with the mean flow as the convective time parameter, T_c. The microscale was achieved by analyzing the properties of a flow field where the viscous and convective time parameters are equal. This condition defines the smallest possible time scale because at this instant, an eddy would be small enough to dissipate into itself before given an opportunity to be affected by or travel with the mean flow. By defining the time parameters as shown below, Kolmogorov then generated the smallest scales of turbulence now known as the Kolmogorov microscale:

Viscous Time: $$T_v = \frac{\nu}{U^2} \qquad (3)$$

Time Scale: $$T_k = \sqrt{\left(\frac{\nu}{\varepsilon}\right)} \qquad (4)$$

Convective Time: $T_c = \frac{L}{U}$ _(5)_

Velocity Scale: $U_k = \sqrt{(v\varepsilon)}$ _(6)_

Length Scale: $\eta k = \sqrt[\frac{1}{4}]{\frac{v^{\frac{1}{3}}}{\varepsilon}}$ _(7)_

Where L = Length
U = Velocity
ν = Kinematic Viscosity
ε = Viscous dissipation

In this microscale viscous dissipation, ε , is a crucial variable as it represents the viscous dissipation rate of the airflow. However, the nature of turbulent flow makes this parameter very difficult to define. Kolmogorov and many other researchers spent several years developing formulas for deriving ε in various engineering flows such as channel flow, turbulent jets, and pipe flow. This research will utilize one of the most direct formulas derived by Kolmogorov in 1952:

$$\mathcal{E} = 15V\left(\frac{DU}{Dt}\right)^2 \quad \text{_(8)_}$$

Since the experiments produce finely detailed graphs of velocity as a function of time, (Du/Dt) can be determined to generate a value for ε.

3.1.3. Spectral Analysis

There are numerous types of turbulent flows, some of which become extraordinarily complex. For years researchers searched for ways to analyze these very convoluted flows until 1947 when Kolmogorov also defined the use of the spectrum

function as a way to further characterize turbulence. Spectral analysis decomposes turbulence into elements that vary harmonically through space and time. The spectrum function specifies a particular superposition of harmonic components with differing frequencies or wavelengths. It gives the variation of a component's intensity with frequency or wavelength. By using a high and low pass filter, one may see the contributions from every part of the frequency range. The lower frequency limit is determined by intrusion of long period fluctuations not directly associated with turbulence. The upper frequency limit is determined by the appearance of electrical noise at high frequencies or by a limitation in the frequency response of some electrical equipment. As a measure of turbulent profiles and activity, Kolmogorov defined the spectrum function that enables the researcher to examine energy versus wave number:

$$E(k)=K_o E_p^{2/3} k^{-5/3} \qquad (9)$$

Where Ko = Constant
Ep = Energy
k = Wave Number

Since spectrum functions are widely used in turbulent studies, this research will rely upon spectral figures to define particular turbulent flows in this clean room study. Upon studying the velocity profiles and their spectral functions, this research will proceed to model the airflow patterns as homogeneously turbulent flow. This type of flow was first defined by H.K. Batchelor in 1948. Homogeneous turbulence has been considered an idealized concept for many many years because there is no known method of exactly realizing such a motion. However, in certain circumstances, departure from exact

independence of fluid properties on position can be small enough to enable a close approximation to homogeneous turbulence. Homogeneous assumptions have been used in the past to treat the flow in the center of a channel or pipe. The data of Comte-Bellot (1965) showed that although such a flow is not homogeneous at low wavenumbers, it becomes more so at higher wavenumbers corresponding to smaller eddies. Taylor's hypothesis also supports homogeneous assumptions by stating that the statistical properties of slowly decaying turbulence carried by a uniform flow are identical to those that would be found by averaging these properties over a large volume of homogeneous turbulence. [9]

Currently, the closest approximation to homogeneous turbulence is described in the flow of a uniform stream passing through an array of holes in a rigid sheet, or a rectangular grid of bars, perpendicular to the stream. The resulting air stream maintains the same uniform velocity with a superimposed random velocity distribution. The random motion dies away with distance from the grid, but the rate of decay is so small relative to the turbulent time scales that homogeneous assumptions are valid. Filtered air is introduced into modern clean rooms in a manner remarkably similar to this approximation.[10] HEPA filters provide an array of holes which are perpendicular to the air stream and generate grid turbulence. They create an air stream that maintains a uniform velocity but with points of random velocity distribution. In clean rooms, the fully developed airflow sustains uniform turbulence in the streamwise direction and the rate of decay can be easily measured.

Introducing the theory of turbulence and its implications enables the dynamic incorporation of particle flow research, which has been long neglected. For instance,

one of the more important issues in clean room modeling is the accurate prediction of particle deposition. Modeling turbulent clean room airflow patterns will facilitate the use of Kolmogorov's microscale to characterize the small eddies in which particles may be embedded. Since the micro-length scale, η_k, determines the relative size of the smallest eddies in turbulence, the study of the eddies may be complemented with Stokes flow analysis to determine possible particle paths and deposition rates in clean room areas. (Stokes flow applies to the individual particles whose motion corresponds to Reynolds numbers less than 1.)

3.2 Particle Deposition

Since the amount of particles in a clean room would be of no interest without their deposition rates, the study of particle probability must include the study of those factors which influence particle deposition. Particle deposition theory analyses gas-particle flows by studying the trajectory of the particles as Stokes flow and treating the supporting air stream as turbulent. Particle flows applicable to this research contain small high density particles whose settling velocity is on the order of the air's root mean squared velocity. Particles of this nature in a gas stream are easily carried by turbulent flows and are dispersed by turbulence.

Once particles are generated and released from their source materials, they may be carried by air currents generated by operator motion or air flow. The controlling parameters of equipment, particle, and airflow determine whether a particle will depose on a surface or follow the streamline around the surface. [11] The relative energy level

between a particle and a probable point of deposition controls the rate at which particles are collected and retained on surfaces. The types of energy gradients most important in clean rooms are electrical gradients generated by process equipment, thermal gradients generated near worktools of increased temperature, and kinetic gradients generated by motion. Electrical gradients may often ionize a particle and attract it to product or equipment surfaces whereas thermal gradients can create buoyancy effects to artificially displace particles into thermal plumes. However, kinetic gradients are by far the most dominant because they are generated by the movement of operators or objects as well as fans. The motion of a particle in a gas flow is governed by gravity and the particle's interaction with the turbulent fluid surrounding it. When analyzing gas particle flows, it is important to remember that these flows are characterized by properties of both the particles and the turbulent gas carrying the particles. The analysis relies on Stokes flow at low Reynolds number for the particles and on high Reynolds number turbulent flow for the surrounding fluid.

Particles may be characterized by their density and their response time, defined as:

$$T_p = \frac{\rho_p D_p^2}{18\mu} \qquad \text{(10)}$$

Where ρ = Particle Density
μ = Fluid Viscosity
D_p = Particle Diameter

When the particle velocity is sufficiently low(relative to the surrounding air flow) to comply with Stokes flow(Re<1), and is dominated by viscous drag forces, the time

required for the particle velocity to decrease to 1/e of its original value is defined as the response time, T_p. The drag on a particle depends on the velocity as well as roughness and surface to volume ratio of the particle itself. Although drag on particle surfaces due to the fluid is much greater than the gravitational force exerted on the particle, near spherical solid particles greater than 10 microns in diameter will settle quickly under gravitational forces. Settling velocity is the velocity given a particle as a result of gravitational forces and is defined as:

$$V_d=gT_P. \qquad \_(11)\_$$

Stokes number, St, is the ratio of the response time of a particle T_P to the time scale of the fluid, T_{ME} (time moving eulerian time scale). Using T_c, the convective time scale of the mean flow, St indicates how closely particles follow the mean fluid motion. Kolmogorov's research illustrated that particles of low inertia have velocity characteristics which coincide with those of gas phase turbulence. Further, when the ratio of the particle diameter to the length scale is less than 0.1, the drag on particles is well characterized by Stokes law. Since particles in clean rooms are well within the microscopic range fitting this criterion, this research will utilize stokes flow to analyze particle motion.

In 1886 Stokes theory attempted to describe the forces acting on airborne particles. The theory defines Newton's second law in the form:

$$m\frac{du}{dt}, = mg = m'g - F \qquad \_(12)\_$$

Where m = Mass of particle = $\pi D^3\rho_p$
m'= Mass of fluid displaced by particle = $\pi D^3\rho_f$

F = Force resisting particle's motion
g = Acceleration of gravity
$\frac{du}{dt}$ = Acceleration of particle

For gas particle flows with (ρ_f/ρ_p)=.001, pressure gradient can usually be neglected, and in most computations, the initial conditions are either zero or go to zero very quickly. Assuming the particle is spherical, and only frictional forces are acting upon it, its motion may be governed by Stokes' equation:

$$F=3\pi\nu U d_p \qquad \_(13)\_$$

Substituting into Newton's equation and assuming a constant particle velocity, an expression for the settling velocity of a particle becomes:

$$V_s = g D_e^2\left(\frac{u_p - u_g}{18q}\right) \qquad \_(14)\_$$

However, clean room particles less than 1.0 micron in diameter will have an increased settling speed because of their tendency to slip between air molecules with little or no drag. For such particles, a correction factor known as the Cunningham-Stokes factor must be applied:

$$V_{corr} = V_s\left(\frac{D_c}{D_p}\right) \qquad \_(15)\_$$

Where D_c = Correction Constant = 1.172 m
D_p= Particle Diameter in microns

Table 3.1 illustrates particle settling rates of various sized particles with applicable Cunningham-Stokes corrections. These figure were obtained by using latex spheres of varying diameter in an operational clean room.

SETTLING RATES OF AIRBORNE PARTICLES*

Diameter of particles (microns)	*Velocity of Settling*		
	Feet per Minute	*Inches per Hour*	*Centimeters per Second*
0.1	0.00016	0.115	0.000081
0.2	0.00036	0.259	0.00018
0.4	0.0013	0.936	0.00066
0.6	0.002	1.44	0.0010
0.8	0.005	3.60	0.0025
1.0	0.007	5.04	0.0036
2.0	0.024	17.3	0.012
4.0	0.095	68.4	0.048
6.0	0.21	151	0.11
8.0	0.38	274	0.19
10	0.59	425	0.30
20	2.4	1,728	1.2
40	9.5	6,840	4.8
60	21.3	15,320	10.8
80	37.9	27,250	19.2
100	59.2	42,600	30.0
200	352	253,500	179
400	498	360,000	253

Table 3.1- Particle Settling Rates

Defining a turbulent clean room model will support very different assumptions of particle generation and distribution within clean rooms. When particles are introduced into a turbulent system, the behavior of the fluid can be changed drastically depending

on the particle density and size; the system has now to incorporate the dissipation due to the particles as well as the behavior of the flow around the particles.

3.3 Results of using current model

By complying with antiquated recommendations for clean room specifications, modern facilities may operate with air velocities as high as 110 feet per minute(FPM).[12] Although this value seems high to the clean room neophyte, those in the industry for several years have used this rigid parameter, among many others, to generate the "Bible" of clean room specifications. Because it is often not examined carefully enough, the original clean room prototype has developed strict paradigms in the minds of clean room engineers. Vertical Laminar flow was so phenomenal an advancement, that few engineers examined this research with a close eye. This has led to the common misconception that higher air velocities produce greater self-cleansing capacities without adverse particle or deposition effects. Although higher air velocities were proven detrimental to conventional clean rooms, many engineers feel they are circumventing air blast issues by adapting VLF. However, upon careful examination, one may see that there is no magic number for air velocities in clean rooms, every facility is unique. Ironically, although the vast majority of researchers continue to use the rigid parameters recommended by the original VLF prototype, few are familiar with the history of these experiments.

In 1962 Sandia's Advanced Manufacturing Development Division envisioned the future of micro-machining. They were the first organization to begin setting design standards and operational specifications for these highly contaminant controlled rooms

now called clean rooms. Sandia first constructed a horizontal laminar flow prototype(HLF), measuring 6 feet in length, 10 feet in width, and 8 feet height, in which to examine the various clean room parameters and generate optimal values. The study initially analyzed airflow patterns in the prototype and then incorporated particulate control.

The room velocity was set to 0 feet per minute and using velocity measurements, was increased until uniform horizontal air streams could be documented. Believing unidirectional streamlines would provide a high self-purging capacity, researchers proceeded to alter air velocities to see the effects on particle counts. They conducted a series of 24 hour tests in which they injected 100 micron diameter particles and collected particle counts at the return grilles. To determine the air velocity which purged particles most efficiently, researchers analyzed their series of collected particle counts and selected the velocity which resulted in the displacement of the most particles at the return. Then, based on room height and width, the prototype research proceeded to suggest a minimum of 20 air changes per hour(ACH) was necessary to purge a uniformly contaminated volume of air. Researchers then developed a full list of recommended clean room specifications which include the magical 110 FPM velocity, 68°F temperature, and 42% relative humidity.

3.4 Critiques of the Current Model

Reasonable criticisms arise when comparing Sandia's research model to modern clean room facilities. Primarily, researchers concluded that higher air velocities yield lower particle concentrations, but neglected to conduct further experiments to find the

influence of higher velocities on higher particle deposition rates. Large flow rates at high velocities will displace a particle to the surface directly beneath it. For most clean room facilities this means particles generated from operators will be literally pushed onto the product. Because particle deposition is a more important factor than particle concentration, today's engineers must consider this concept before regulating clean room air velocities.

Sandia determined optimal air velocities by using 100 micron diameter particles in their prototype. Perhaps this particle size was indicative of the particles emitted by the older overgarments of the 1960's. However, today's clean room garments provide cleanliness levels up to 2 orders of magnitude higher by preventing the emission of particles over 1.0 micron in diameter.[13] The factors which effect large particles in the flow stream in general do not coincide with those governing small scale particulate motion. These large particles are insusceptible to Brownian motion, are more easily influenced by gravitational forces and their subsequent motion is more easily effected by drag. Gravitational forces drive large particles more rapidly towards the floor at rates proportional to their size. Additionally, horizontal flow clean rooms entirely neglect the gravitational effects of vertical flow clean rooms. Since gravitational effects aid in the removal of particles, clean room air velocities could be considerably lower than Sandia's optimum. Also, the larger surface areas of large particles makes them more readily effected by drag. Sandia's horizontal flow clean room did not account for these phenomena and could have quite easily over estimated their reference velocity as a result. Moreover, particle counters are notorious for their exclusion of large particles. Because particle counters previously measured particles by their projected area on

internal witness plates, they often recorded large particles at smaller sizes. Thus, studying the aerodynamics of particles 100 times larger in magnitude than those actually in the clean room, will certainly yield misleading results. Next, one must consider the validity of the prototype's assumption of uniform particle generation and distribution within clean rooms. In today's workplace, particles generated from operators or equipment are localized; operators are dynamic and process equipment transient. Increasing air velocity will indeed purge the room uniformly, but does little to the area where particles are concentrated. Research from the 1993 ASME Gas Particle Flows Symposium indicates that particle concentrations and collisions peaks occur near the viscous wall region because of thermal gradients and electrostatic effects[14]. When air hits the wall, friction effects will reduce its velocity. As a result, particles will traverse more slowly in the wall region and build up larger concentration in this area. The particles' tendency to accumulate in this region results in particle concentrations up to twice the order of magnitude of that in the room's center. Hence, using a uniform particle distribution in this instance will also yield over estimated results.

Ironically, perhaps the largest factor overlooked by current researchers is Sandia's laminar treatment of the prototype airflow. The 1993 ASME research proceeded to suggest that concentration levels in the wall region are closely related to the structure of air flow turbulence. As discussed earlier, the dispersion of particles in the air flow are strongly effected by turbulent eddies generated by higher air velocities. Faster moving eddies have been documented to embed and retain particles for up to 30 minutes, possibly displacing them into critical areas[15]. By overlooking the effects of the velocity fluctuations and subsequent turbulence intensities, Sandia oversimplified their

prototype model which casts doubts in their subsequent recommended optimal values. Hence, close scrutiny of the rigid parameters imposed on most clean rooms today illustrates the need to adjust air velocities to meet specific clean room needs rather than set fixed values.

Over estimated velocities have resulted in gargantuan facilities which often consume most of a community's natural resources. From a facility standpoint, the energy costs are proportional to the cube of the air velocity[16]. Higher velocities result in larger air handler units and higher make up air requirements. Furthermore, larger equipment and subsequent capacities result in larger redundancy specifications. From an engineering standpoint, this can be avoided as studies from Particle Measuring Systems have shown that filters producing a 90FPM face velocity are as efficient as those producing 50FPM. Additionally, many engineers believe that larger air velocities will not only flush out particles more efficiently, but also remove particles from surfaces. However, further studies from PMS have proven that clean room airflow must travel at speeds close to Mach 1 before they are capable of removing particles from surfaces. Hence, there are numerous misconceptions often mandating engineers to build clean rooms at 90FPM unnecessarily. To illustrate how clean rooms may still comply with Federal Standard 209E and maintain unidirectional airflow at lower velocities, this research will conduct experiments measuring the velocity profiles and subsequent particle counts and distributions at these lower velocities.

Chapter 4

4.1 Experimental Model and Setup

This research will measure the velocity profiles of three separate air velocities, 50FPM, 70FPM, and 90FPM, in an operating class 10 clean room. Velocity measurements will be taken with 8 hot wire anemometers placed on 4 different levels, A,B,C, and D. Turbulence intensities of each level will be determine the vertical and horizontal characteristics of each air stream. Afterwards, injected particles will measure deposition rates with the use of test wafers and a wafer inspection station. The anticipated results will illustrate different turbulent zones in the four levels and an increase in particle deposition rates with higher air velocities.

This research utilizes the support facilities of MIT's Microsystems Technology Laboratories (MTL). An 8 by 10 by 8 foot grid section of the Technology Research Laboratory(TRL) was isolated for this research. The TRL facility is equipped with 2,000ft^2 of class 10 clean room space, sustains 95% HEPA coverage and uses a pressurized plenum arrangement for the introduction of clean air. The facility does not implement perforated flooring but instead utilizes a large surface area of floor and side wall return grilles.

As shown in Figure 4.1, the experimental area encloses nine HEPA filters and one blank panel, as well as two wall mounted return grilles and one floor grille along the area's length. Since the area lacks hard wall partitions between itself and the isleway, visqueen along the area's perimeter simulated hard walls during experiments. The experimental grid is divided into 15 data points and its size is limited by exhaust and utility connections of an adjacent acid wet station and analytical equipment. The grid

provides the study of airflow patterns in the center, floor return, and a side wall return regions.

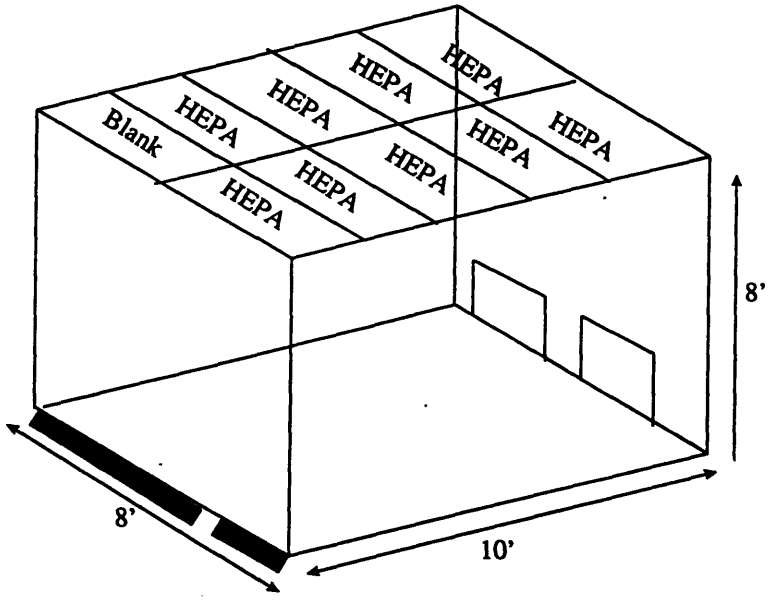

Figure 4.1-Test Grid

4.2 Hot Wire Anemometry

This experiment will characterize the nature of clean room turbulent flow by gathering data depicting the velocity profile. In order to measure fluctuating velocities at varying spatial points, the research will utilize hot wire anemometers for their high frequency velocity response. Since hot wires sustain frequency responses in the kilohertz range, they are widely used for turbulence measurements in gas flows. The underlying theory of hot wire Anemometry may be explained in very pragmatic terms. Heat transfer theory proves that an object traveling through an air stream will lose heat in a manner proportional to its air velocity and reach a temperature determined by the

rate of cooling. From this premise, it is relatively straightforward to correlate an air stream velocity with a corresponding voltage drop in given a power supply as shown in Flow Chart 4.1:

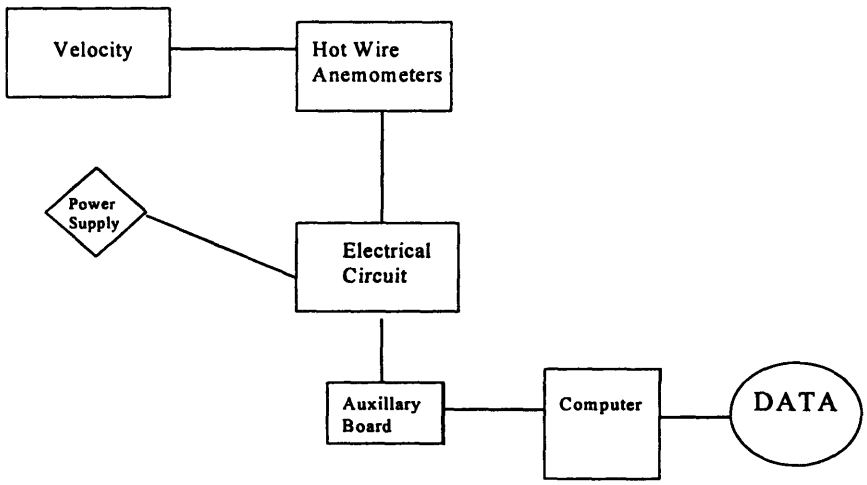

Flow Chart 4.1- Anemometer Concept

The hot wire anemometer probe measures the heat transfer by delivering a measurable electrical current to a very thin variable resistance wire held by metal supports. Figure 4.1 shows the device in cross section:

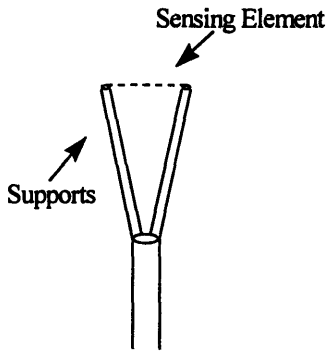

Figure 4.2- Hot Wire Anemometer Probe

Since this research is using hot wires to measure the smallest velocity fluctuation which characterizes small scale turbulence, the sensing element(wire) must be much smaller in length than the smallest eddy possibly measured. As a result the sensor is very fine measuring 1 millimeter in length, and 0.5 microns in diameter. Because the wire changes its resistance with temperature to facilitate electrical analysis, it is important to consider buoyancy effects near the wire which effect data by generating artificial flows. The overheat parameter is a measure of the wire's temperature compared with that of its ambient and is defined in the following relation:

$$a = \frac{R_w - R_0}{R_w} \qquad \text{(16)}$$

Where R_o = cold resistance
R_w = wire resistance

The overheat parameter allows the researcher to consider the magnitude of free convection effects near the wire and compensate for them. The typical value in air streams of 80% was used in this experiment. Assuming static equilibrium, the following energy balance is proposed:

$$\frac{dE}{dT} = (W - H) \qquad = 0 \qquad \text{(17)}$$

Where E = Thermal energy stored in the wire $= C_w T_w$
W = Electrical power $= I^2 R_w$
H = Heat transferred to surroundings $= hA(T_w - T_f) + K(Dt/Dx) + \varepsilon\sigma(T_w^4 - T_f^4)$

Thermal energy is represented as a temperature dependent function of the wire's heat capacity, C_w, and its temperature while electrical power is represented as the square of the current multiplied by the wire resistance. Heat transferred to the surroundings includes convection to the fluid, conduction to the supports and radiation to the ambient. With cylindrical wires, the convection effects are measured by the heat transfer coefficient, h, times the temperature difference, the conduction by the thermal conductivity, K, times the temperature gradient and the radiation by the Boltzman constant, σ, times the difference of the temperatures to the fourth power.

By the nature of this instrument, it is important that probe casings and body are slender enough to prevent interruptions in the flow around the wire, but also rigid enough to prevent wire vibration. In doing so, hot wires require prong supports which are more massive than the wire and unfortunately leads to increasing conduction effects with heat loss from the wire to the prongs. However, keeping the wire's aspect ratio, length over diameter, at approximately 200 will limit these effects[17]. Radiation effects become important when there is a large temperature difference between the wire and the ambient. Because the effects follow as the temperature difference to the fourth, heat transfer effects may be significant. However, radiation effects are safely assumed to be less than 10% of the total heat transfer in normal applications. Thus,

with hot wire anemometry, forced convection associated with the heated wire can cause significant vertical movement of its adjacent fluid. The severity of buoyancy effects are indicated through the flow's Grashof number, Gr. Previous research in hot wire anemometry suggests that if the flow's product of Grashof number and Reynolds number is less than 10000, it will generate insignificant free convection effects near the wire. However, recent research from Leinhard at MIT[18] indicates a less stringent criteria which states that flows with Grashof numbers less than their corresponding Reynolds number to the third power, have negligible free convection effects. Hence, the minimum velocity reliably measured with hot wire anemometry is that which is equal to the free convection created by the wire. In this case, free convection is limited to velocities under 0.1m/s. Since this research will operate within these constraints, free convection effects near the wire will be neglected.

One crucial heat transfer consideration in hot wire anemometry is the effect of the wire's yaw and pitch angle. As shown in figure 4.3, a three dimensional flow will enable velocity measurements at different angles in the three planes. The yaw is the angle incident to the wire in the plane parallel to the supports, while pitch angles are measured in the plane perpendicular to the wire and supports. Altering yaw or pitch angles will change the velocity vector incident upon the wire and in so doing effect the heat transfer. Since the device will primarily measure the velocity component perpendicular to the wire, it will return lower values for yawed velocities because it can only measure the projection of the velocity vector in this plane. At first glance, pitched velocities would not seem to effect the heat transfer since the vector is always perpendicular to the sensing element. However, the 1993 ASME Symposium on

Thermal Anemometry indicates that placing supports perpendicular to a mean flow may causes wakes near the wire resulting in more heat loss to supports and a higher output from the probes[19]. Although some may argue that pitch effects are minimal, velocity readings may be easily adjusted using corrections called K factors. Yawed velocities produce first order effects and are corrected by K1 factors while pitched velocities produce second order effects and are corrected by K2 factors. Both factors depend on individual angles and velocities however yaw angles require more stringent corrections on the order of 20% while pitch angles require a correction of only 5%. Because these experiments utilize the devices configured at a 90^0 pitch and 0^0 yaw, the output voltages will be corrected by roughly 5%.

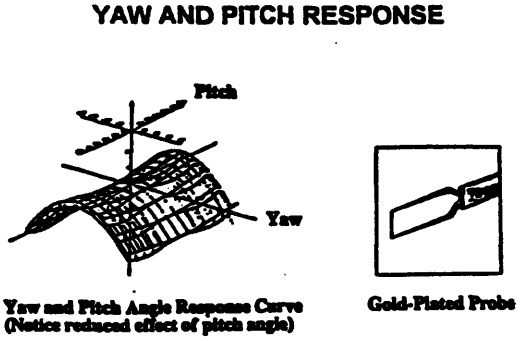

Figure 4.3- Yaw and Pitch Angles in Hot Wires

Proceeding with the assumption that convection effects dominate, and device configurations do not significantly alter the energy balance, the static equilibrium equation reduces to the following:

$$I^2R_w = hA(T_w - T_f) \qquad \_(18)\_$$

These relations establish how heating current is used as a measure of velocity. Hot wire anemometers determine a flow's velocity through the circuit's corresponding output voltage. A Wheatstone bridge and high gain servo amplifier are used to drive this research's devices. The circuit is initially balanced with the "cold" wire but designed to react quickly as velocity fluctuations alter the wire's resistivity and cause voltage imbalances in the circuit. W, the joule heating in this circuit, can now be more accurately represented as:

$$W = I^2R_w = E_w^2 = R_w(R_w - R_a)(C_5 + C_6\sqrt{U}) \qquad \_(19)\_$$

Where E_w = Voltage
C_5, C_6 = Constants

Since the experiments must measure accurate velocity fluctuations, numerous electrical stages were needed to boost the electrical signal. Unfortunately, Dantec Technologies has documented that use of 12 bit A/D converters in most hot wire anemometer applications will yield noise levels equivalent to a 2% turbulence level.[20]. Since this experiment anticipates velocity fluctuations within 1.0% of the free stream velocity, several control measures must be implemented. Because air velocities in clean rooms are on the order of 0.5 m/s, velocity fluctuations at .05m/s border the minuscule and a series of high gain Operational Amplifiers(Op-Amps) are essential in the anemometer circuitry. As shown in Figure 4.3, the experiments utilize Constant Temperature Anemometers(CTA) by supplying a constant voltage sustaining a constant hot wire temperature.

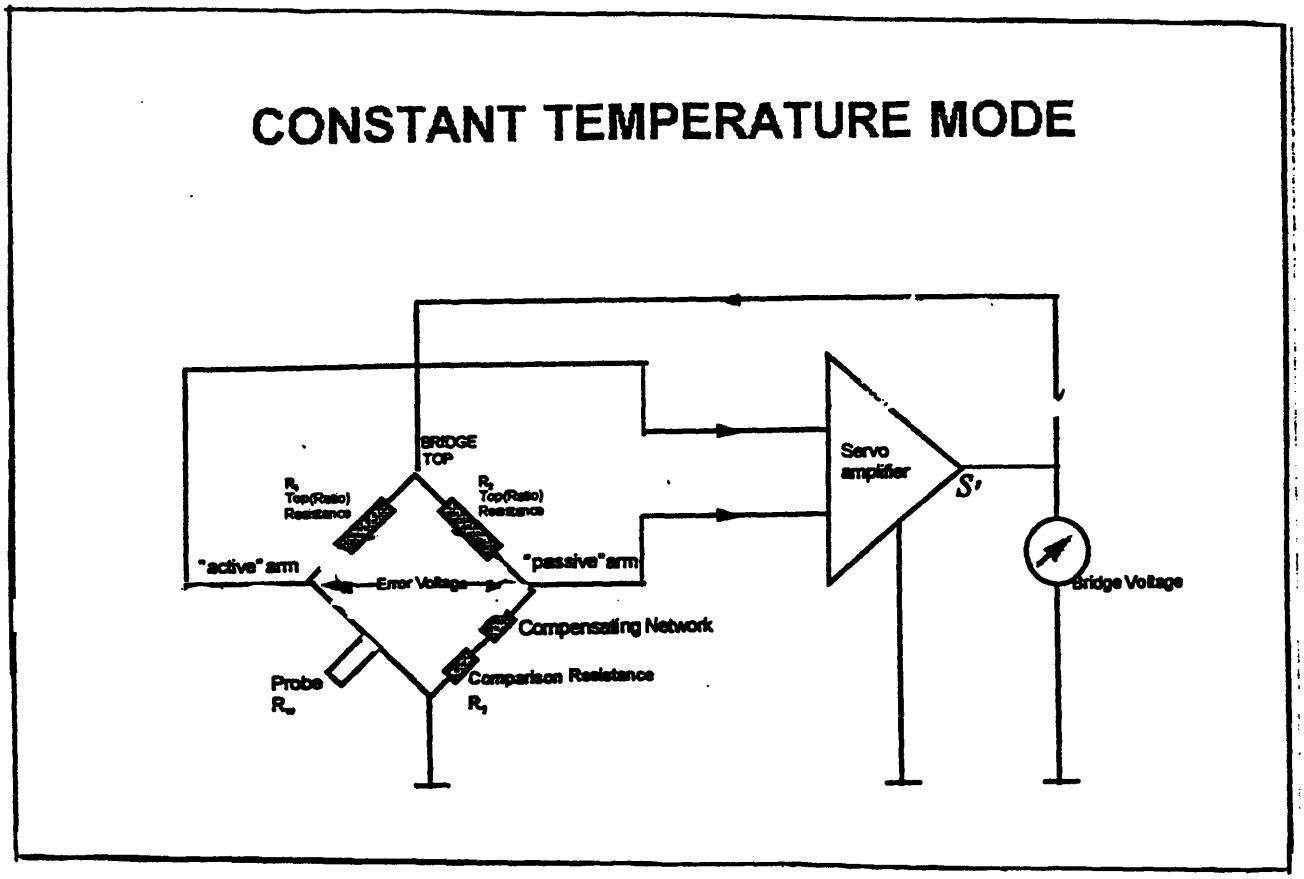

Figure 4.4 - Electrical Circuit

The required resolution and magnification of the output signal are accomplished through various Op-Amp stages within the Servo Amplifier: Input and Output(I/O) Buffers, Multipliers and Scalers. Each probe retains its own corresponding electrical circuit consisting of 10 resistors, 6 Op-Amps, and 2 potentiometers. One potentiometer serves as an input bias while the other is utilized as an output bias. These variable resistors must regulate the input and output voltages corresponding to a specific probe's resistivity. The bridge formed by these potentiometers essentially functions as a control system for probe resistance, maintaining the resistance in response to changes in convective cooling by varying the voltage across the probe. The time varying voltage

signal associated with maintaining the wire resistance at the level determined by the overheat ratio constitutes the primary output of the bridge amplifier system.

Although the circuit will balance itself extremely quickly, because the control system is defined by a differential equation, the wire's thermal lag will yield a finite velocity response of:

$$Y(f) = \int_{-\infty}^{+\infty} Y(t)\, e^{-2i\pi ft}\, dt \qquad \text{(20)}$$

By dividing the output function by the input, the system transfer function may be determined as:

$$H(f) = \frac{K_{ct}}{1 + j\omega T_{ct}} \qquad \text{(21)}$$

Where T_{ct} = Frequency Response: $T_{ct} = \dfrac{T}{2aS' R_w}$

S' = Amplifier gain

a = Overheat parameter

The time constant, T_{ct}, defines the frequency response of the system which will be on the order of 25Khz for this experiment. As a result, a sampling rate of 100kHz was used in an attempt to characterize the smallest time scales. One important consideration is that the spatial resolution of the response be proportional to the sensor dimensions. The circuit cannot resolve scales smaller than the wire diameter and will hence be limited in its frequency range.

4.2.1 Probe Calibration

Despite extensive work, there exists no universal expression to describe the heat transfer from hot wires. It is for this reason that all actual measurements require direct anemometer calibration. Initial and frequent calibration is essential with every hot wire usage because it enables the researcher to produce reliable data from the conversion of experimental measurements. Since high level fluctuations often influence the measured voltage across hot wires, it is advantageous to calibrate probes in low turbulent flows. As a result, this experiment's probes were dynamically calibrated in the velocity range of their anticipated usage using a low turbulence wind tunnel. Given the nature of clean room air velocities, it would be advantageous to calibrate the probes at the smallest velocity possible. Although clean room crossflows may approach 0.2m/s, the wind tunnel motor could overheat at velocities lower than .28 m/s, forcing the use of a 0.3m/s-0.8m/s range instead. By varying the wind tunnel airspeed, known air velocities are directly correlated with output voltages. King's Law results in voltage-velocity curves shown in Figures 4.3(a)-(h):

$$V^2 = A+Bu^n \qquad \_(22)\_$$

Where A,B = Constant

n = Velocity Exponent

Figure 4.3(a) – Calibration curve for probe 1

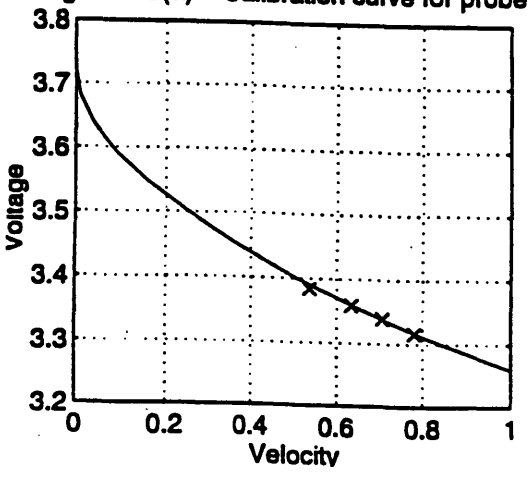

Figure 4.3(b) – Calibration curve for probe 2

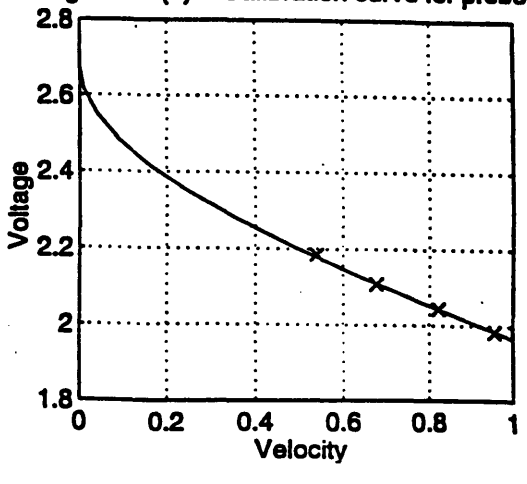

Figure 4.3(c) – Calibration curve for probe 3

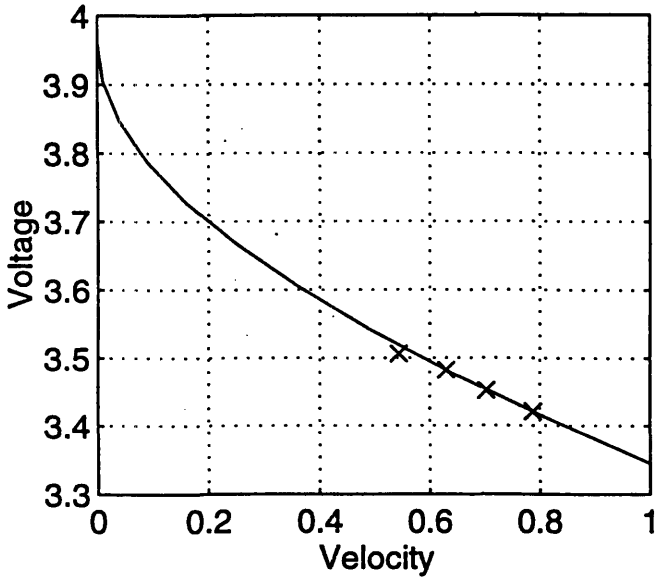

Figure 4.3(d) – Calibration curve for probe 4

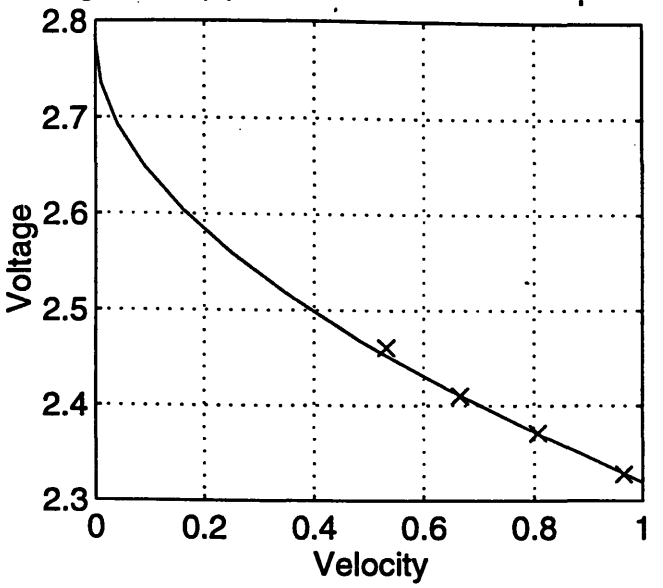

Figure 4.3(e) – Calibration curve for probe 5

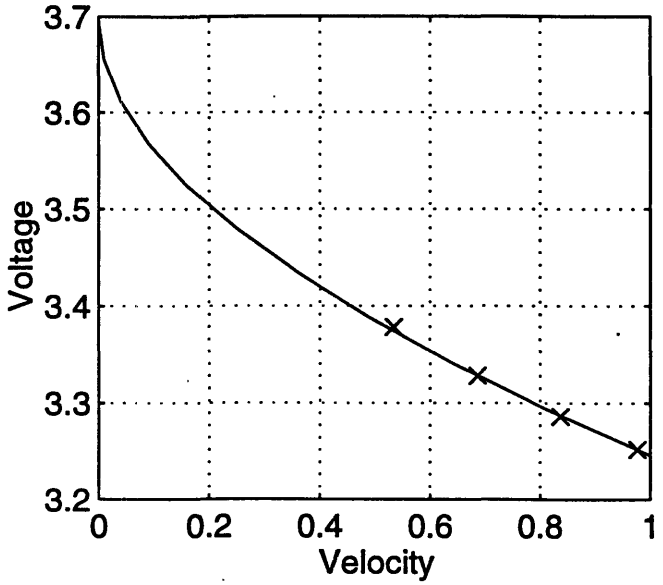

Figure 4.3(f) – Calibration curve for probe 6

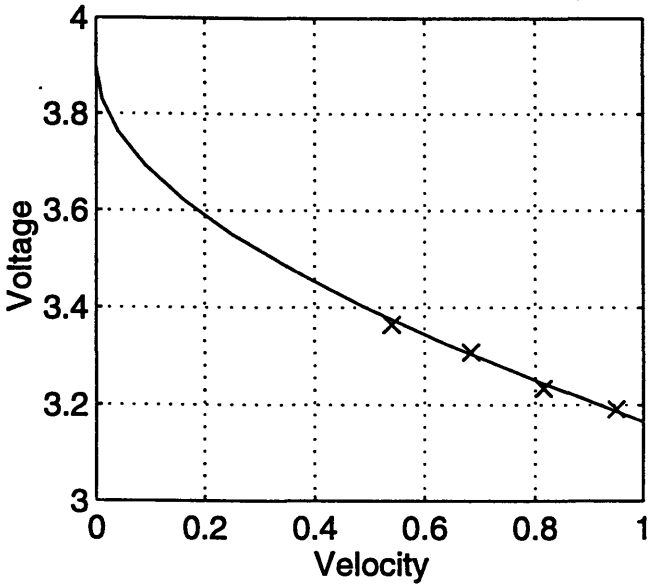

Figure 4.3(g) – Calibration curve for probe 7

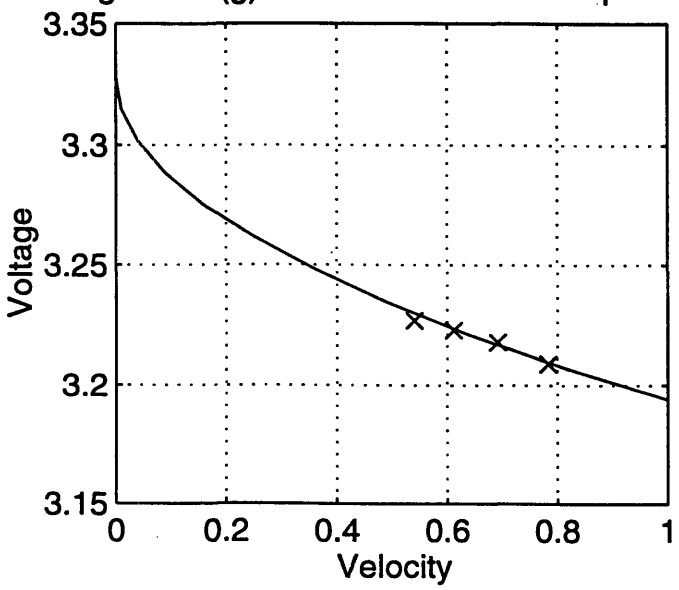

Figure 4.3(h) – Calibration curve for probe 8

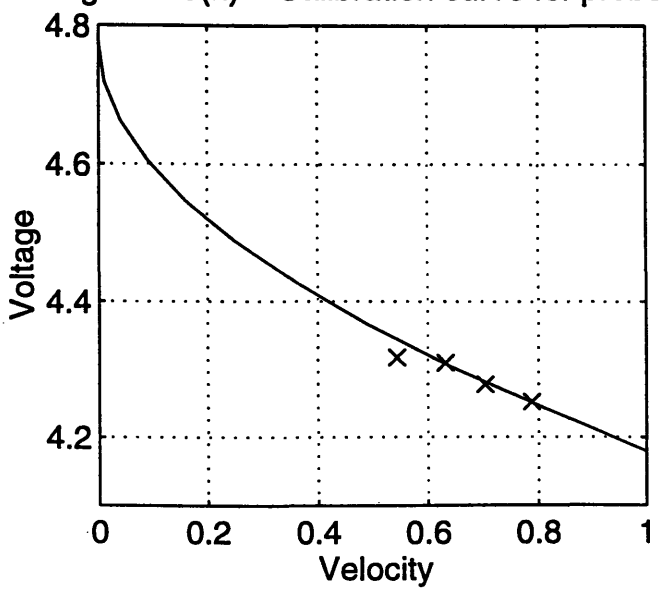

Further research on King's law has illustrated the velocity exponent increases with lower velocities. Hence, although recent papers have suggested n = 0.45 as the better exponent, this research used the standard n = 0.5. Although this relation is among the most standard for hot wire calibration, it retains some inherent impracticalities. For instance, the constants A and B must be determined given input voltages and corresponding velocities. However, one cannot easily set zero voltage as a means to determine A because natural convection effects make it nearly impossible to obtain a true zero velocity. Further, the uncertainty due to natural convection is neither evident in velocity nor voltage. Additionally, a linear least squares fit is inapplicable because King's law is not linear and a higher order polynomial lends itself to further errors. These may be sources of error in the data.

As hot wires respond to convective cooling with a fluctuation in voltage, they transmit this output to a data acquisition unit. A Metrabyte DAS16G Internal Analog to Digital(A/D) converter and an Intel 486SX CPU was used to gather data throughout this research. The A/D board can receive up to 16 channels of unipolar signals. It receives signals between +0V and -10V but represents each voltage as number between 0-4095, where 1 bit represents approximately 2.25 milivolts. A short cable connector attaches the A/D board to a smaller auxiliary board where screw terminal connections receive output voltages from the individual circuits and transmit them to the A/D board for data collection; the signal to noise ratio was measured to be 6:1. Figure 4.5 illustrates the experimental setup:

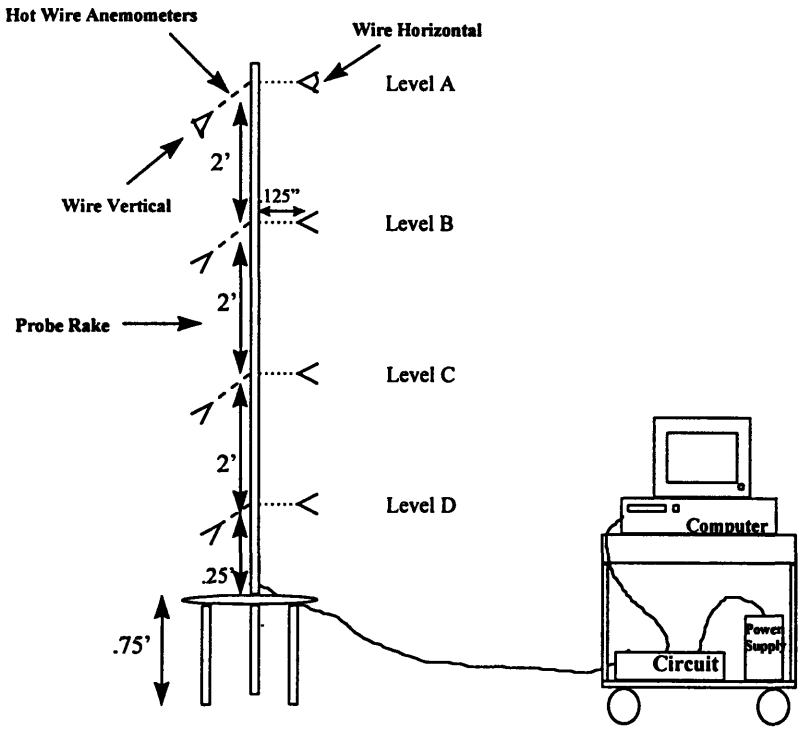

Figure 4.5- Experimental Setup

Since hot wire anemometers are delicate apparatuses which may be easily destroyed by excess vibration or direct contact, they are mounted onto a probe rake for protection during experiments. The probe rake is a steel L-shaped pole 7 feet in height containing one millimeter diameter holes spaced one half inch apart on its sides. The need for adjustable probe locations contributed to the rake's distinctive geometry as these perforations allow probe locations on any level. The hot-wire anemometer probes are placed 2 on each level at 1ft, 3ft, 5ft, and 7ft elevations. In order to measure vertical velocities, odd numbered probes are aligned such that their wires are horizontal, perpendicular to the probe rake. These wires are also perpendicular to the 10 foot length of the room, see figure 4.1 The wires of the even numbered probe are aligned

vertically, that is parallel to the probe rake in order to measure crossflow velocities. The 2 foot spacing was chosen corresponding to the length of the HEPA filter. This research anticipates that clean room flow fields will change with distance from the air source in sections equal to the HEPA's cross dimension.

Probes in the same plane sit perpendicular to each other to best facilitate two dimensional velocity measurements as well as prevent contact between probes. The probe rake containing all 8 hot wire anemometers is moved along the various grid points to determine a velocity profile. The probe heights were chosen such that different probes will yield velocity profiles corresponding to different flow fields. Probe 7 and Probe 8 are placed at the highest level, Level A, located only 8 inches below the HEPA. Due to the eddies generated by HEPAs, the velocity profiles from these probes are anticipated to be homogeneously turbulent. Probe 5 and probe 6, are located 3 feet from the ceiling, on Level B, and should detect a decaying but unidirectional flow field. Likewise, probe 3 and probe 4 are located on Level C, 5 feet from the ceiling, and should depict a deteriorating flow field with increasing crossflow. Probe 1 and probe 2 are in Level A, placed 7 feet from the ceiling(1 foot from the floor) in a region where crossflow currents should be very strong and unidirectionality dissipated.

By moving the probe rake along the grid points, the effect of each flow pattern near the center, floor exhaust and side wall exhaust are shown. Before each test, the air flow is left undisturbed for 5 minutes to achieve steady state. Afterwards, velocity readings are taken for one minute at a 100kHz sampling rate. Probes and circuitry are tested periodically before and after each test. The results will depict velocity profiles of three clean room air velocities: 50 FPM, 70FPM, and 90FPM.

4.3 Humidifier and Particles

Upon measuring airflow patterns, the experiment proceeds to study how each pattern effects airborne particulates. To accomplish this, particles are injected into the experimental area and their deposition monitored. For more accurate results, particles injected into the experimental area should closely resemble the types of particles emitted by clean room personnel during normal operation. However, with the diversity of particles possible, it is impossible to determine what size particles are emitted where. To make this process proceed more smoothly, the industry has adopted the practice of using spherical particles when studying the dynamics of clean room particulates. These particles are injected in a manner consistent with clean room certification specifications. (Although the particles are not intended to challenge the HEPA filters themselves, the procedure is still a useful one for its particle injection techniques.) This experiment utilizes 0.499 micron diameter particles made of polystyrene and certified by the National Institute of Standards and Technology. One 15 milliliter vile of particles, at 0.1% solid, is combined with 1000 ml of water to generate the particulate stream. This mixture is placed into a standard non heating, non purifying humidifier and displaced into the clean room at a 45^0 angle from the horizontal at a rate of .075 milliliters per second in the form of a vaporous spray. This rate was verified by calibrating the humidifier and comparing it to the manufacturer's specifications. The humidifier unit was filled to capacity, weighed, and then operated in four 2 minute intervals. After each test, the unit's weight was compared to its initial value which resulted in the corresponding flow rate. The four test trials demonstrated a consistent pattern with a standard

deviation of 1.73%. The humidifier is then positioned in each of the three test regions, center, floor return and sidewall, return for each velocity. The humidifier mist introduces particles for 90 seconds and is then shut down for 120 seconds to allow particle settling and deposition as well as exit through return grilles. This procedure introduces $7.4x10^4$ particles into the experimental area with each particle spray. Three perimeter wafers permit deposition analysis afterwards.

Based on visual observation, the humidifier's dispersion rate of .075ml/s is able to produce a flow plume that is 30 inches in diameter when passing through the plane containing the wafers. In order to study the deposition of particles at different air velocities, three clean 6 inch wafers are placed around the humidifier's perimeter 20 inches away from the nozzle and 20 inches apart from each other as shown in Figure 4.6:

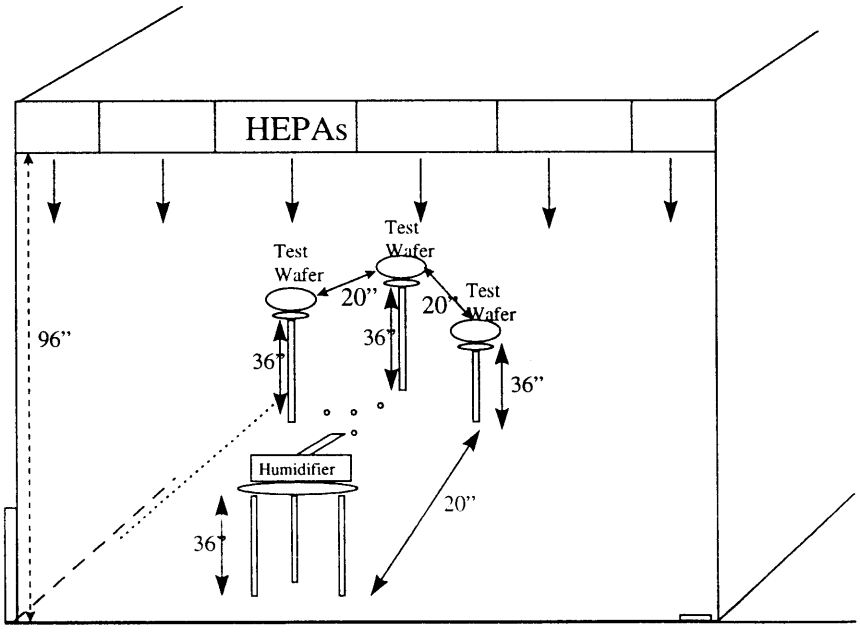

Figure 4.6(a)- Humidifier and Wafer Location

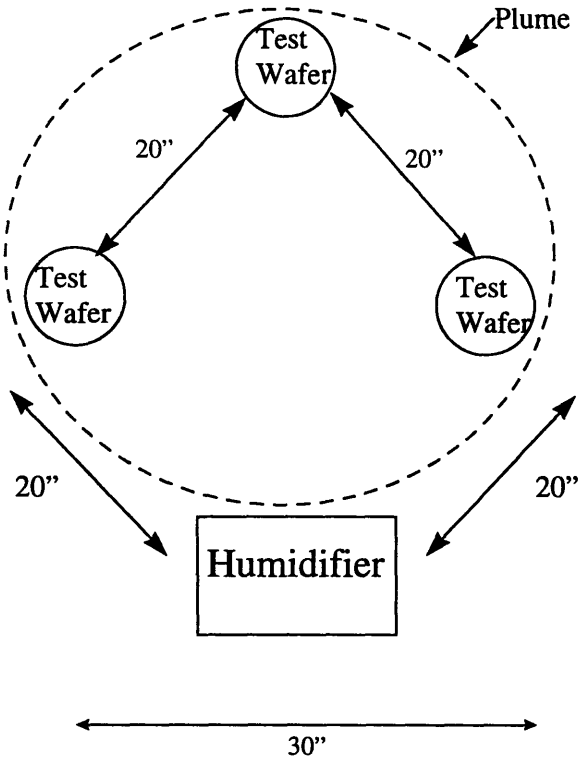

Figure 4.6(b)- Plan View of Test Wafers and Humidifier

The wafer surface area accounts for only 1/25 of the plume area but should catch significant particles. This procedure is performed at the center of the experimental space, near a side wall grille, and near a floor grille for the three identified velocity profiles. After particle injection, the test wafers are carefully removed with nitrogen vacuum wands, so as not to artificially contaminate their surfaces, and placed into an inspection station.

4.4 Wafer Inspection Station

Once particles depose onto a wafer surface, a Wafer Inspection Station(WIS) can produce a particle count, size and distribution on each wafer, see Figure 4.7. Since particles are three dimensional objects, they can be described by their volume, their cross sectional area, their largest dimension or an arbitrary dimension advantageous for the research. The choice is a function of the product the particle will contaminate, and as a result, various methods are used to measure quantity of matter. For instance, in the semi-conductor industry the particle's largest dimension is of interest because of the sensitivity of the wafer. However, in the bio-pharmaceutical industry, the nature of bacteria and other biological products, as well as the strong effect of electrostatics on these materials, require monitoring of a particle's projected area. The Wafer Inspection Station(WIS-100/150) will describe this experiment's particulate matter in terms of its size and distribution on the test wafer. The WIS-100/150 uses a spot laser scanner to sweep a beam of light .003 inches in diameter across the wafer surface.[21] Channel detectors collect and scatter light from the wafer surface to produce frequency and amplitude distortions in light. Since the amplitude is proportional to the size of the wafer's surface flaw, particle size and distribution are easy displayed within 1% accuracy. Table 4.1 shows the flaw descriptions.

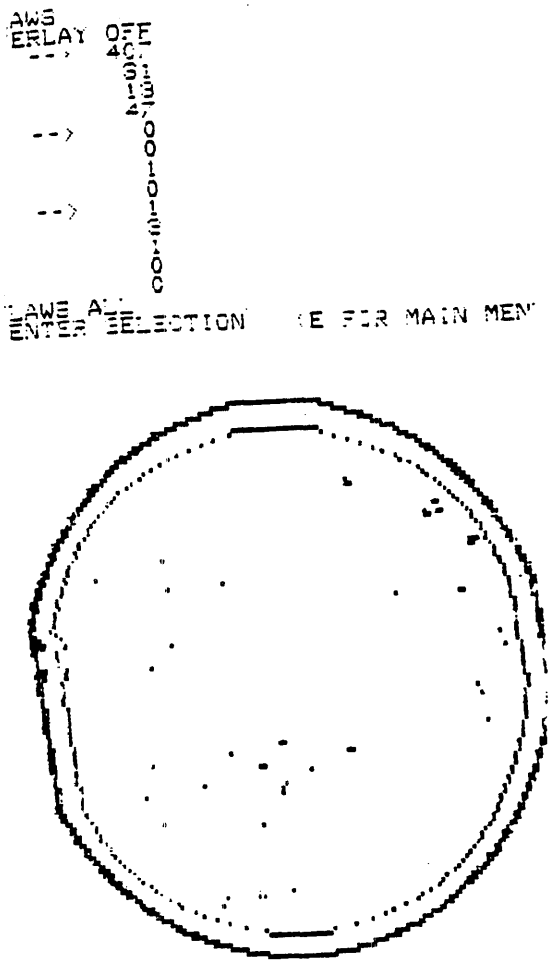

Figure 4.7 - Wafer Output

FLAW NUMBER	DEFECT (THRESHOLD UTILIZED)
1	Haze (T-1).
2	Small pits and particulates (0.3 to 2 microns) (T-2).
3	Larger pits and particulates (2 to 20 microns) (T-3).
4	Cumulative sum of 2,3,A,C, and G defects. Totalizations of particulates.
5	Scratch count. 1,2, and 3 defects in a minimum of four adjacent pixels are converted to 5's and analyzed for scratches.
6	Area defects.
7	Light orange peel, partially polished out saw marks, generally low level and frequency (T-4).
8	Distortion with abrasion such as an unpolished out saw mark (T-4 and T-3).
9	Distortion defects of higher frequency such as small dimples, grooves, and mounds (T-5).
10	(A) Large particulates (T-5 and T-3).
11	(B) Heavy orange peel and related defects (T-5 and T-4.)
12	(C) Severe dirt, abrasions, or film (T-5, T-4, and T-3).
13	(G) Number of edge types not resolved. Also very large defects (T-7).
14	Not currently used.
15	Not currently used.
16	Not currently used.

Table 4.1- Wafer Flaw Descriptions

4.5 Concentration meter

Before placing clean test wafers in the experimental area, a PMS-126 concentration meter will verify the quantity of pre-existing particles. This safety precution reflected zero pre-existing particles in the clean room which indicates the majority of particles on the test wafers are the experimentally injected ones. The PMS-126 concentration meter utilizes a small vacuum wand to extract air from a desired area and count the airborne particulate contaminants within it. The concentration meter deciphers particle size and sorts them into different concentration categories. The PMS-126 is limited in that it may detect particles as small as 0.1 microns in diameter, but cannot distinguish those greater than 5.0 microns. However, since particles less than 1 micron in diameter are the only variety in clean room facilities, this particle counter was sufficient for this research.

Chapter 5

5.1- Statistical and Spectral Results

Statistical and spectral analysis were applied to the experimental results in order to identify regions of homogeneous turbulence. The experimental results indicate there are regions which comply to the assumptions of homogenous turbulence and regions which do not. First, the measured velocity fluctuations were plotted to obtain a probability distribution consistent with the "random" characteristics of homogeneous turbulence. As seen in Figure 5.1, the statistical data tabulated at the center regions of the three velocity profiles depicts the normal distribution of homogeneous turbulence at both Levels A and B:

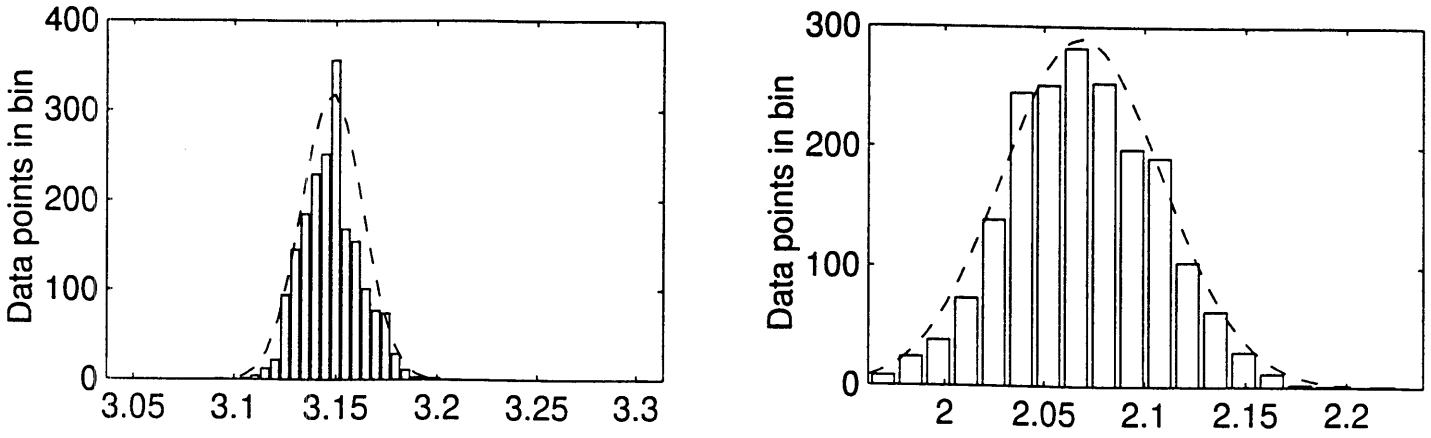

Figure 5.1(a)- Statistical Properties of the 50FPM Velocity Profile;Levels A and B

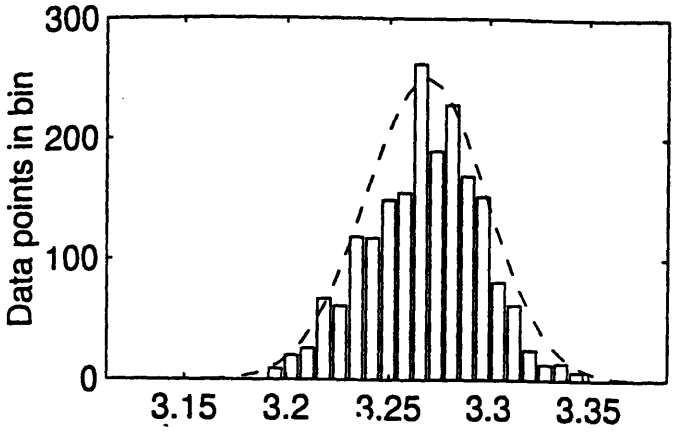

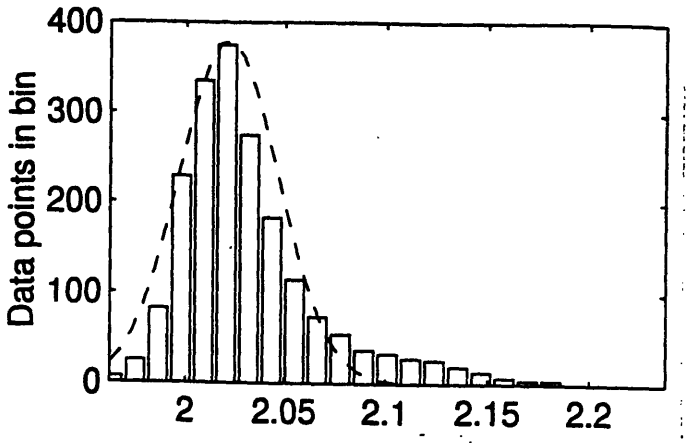

Figure 5.1(b)- Statistical Properties of the 70FPM Velocity Profile;Levels A and B

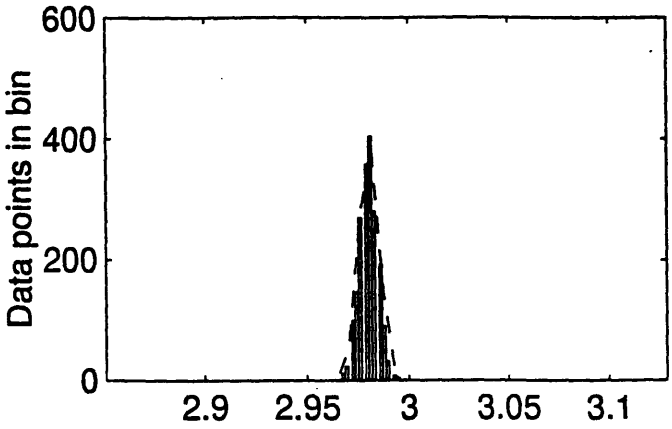

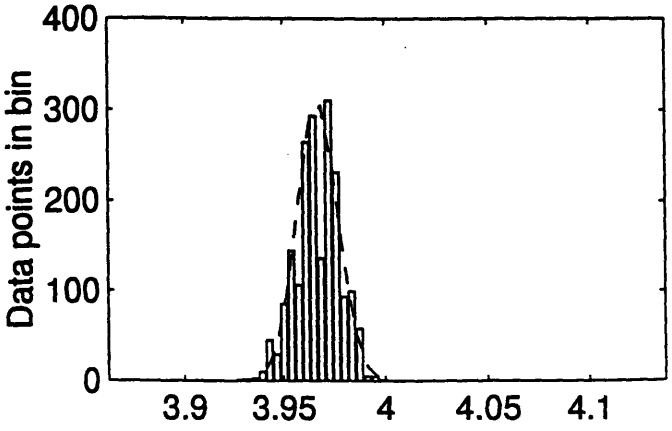

Figure 5.1(c)- Statistical Properties of the 90FPM Velocity Profile; Levels A and B

This data is the first step in demonstrating the existence homogenous turbulence in the three velocity profiles up to level B, half way from the ceiling to the return. Below this level however, the airflow dissipates into other forms of turbulence which cannot be easily categorized by this research.

Figure 5.2 further characterizes the turbulent flow through the use of spectral analysis. One distinctive characteristic of homogeneity is the so called 5/3 law. When Kolmogorov defined the spectrum function as a means to characterize turbulent flows, he paid particular attention to the most ideal case of homogeneous turbulence. By correlating the self-preserving characteristics and the generated mesh turbulence, Kolmogorov concluded that the spectral functions of homogeneous flows will display a decreasing slope of 5/3 in the frequencies corresponding to the flow's smallest turbulent time scale. The data gathered at the center test region illustrated high noise levels in the lower wave number ranges. As a result, the curve's slope was determined using the signal to noise ratio of 6:1. Only the data points a fraction 1/6 above and below the mean value were used to determine the slope of the line. Within the experimental section of the clean room, the slope of the spectral graph was identified as 5/3 with corresponding frequencies beteween10^2 and 10^5 Hz .

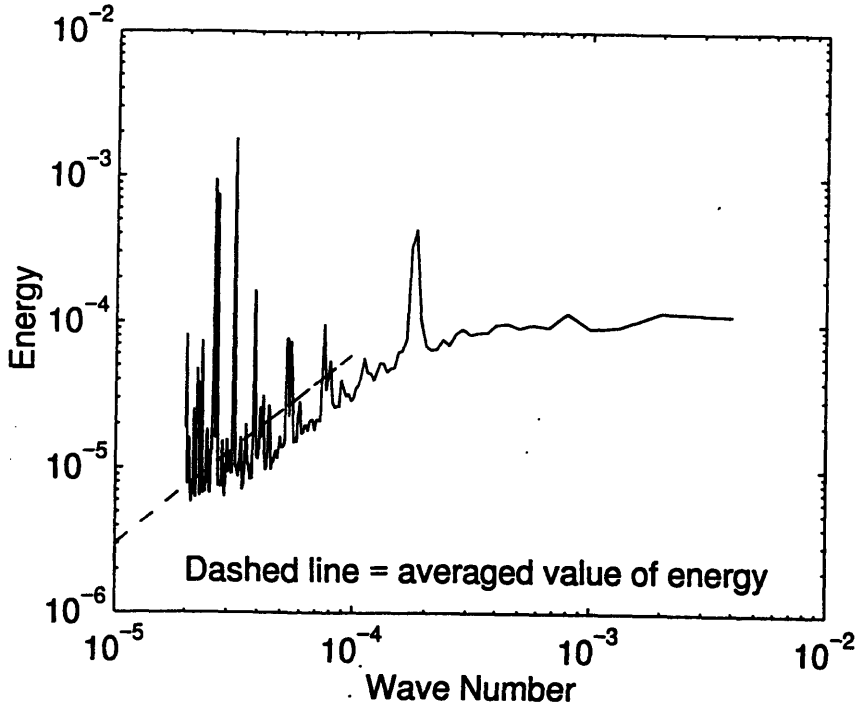

Figure 5.2 - Spectral Analysis

During these experiments, the center test regions of all three air velocities exhibited homogenous turbulence up to Level B, midpath. After this level, however, crossflow velocities were too strong to maintain unidirectionality.

5.2- Turbulence Intensities

Since analysis of turbulent intensities helps identify regions of unidirectionality, turbulence intensity plots of the vertical and horizontal velocity components were generated for the three test regions. Figures 5.3(a)-(c) depict the averaged vertical and horizontal turbulence intensities in the center regions of the 50FPM, 70FPM,and 90FPM velocity profiles. The brackets indicate the standard deviations which were +/- 5% and +/-9% in the vertical and horizontal intensities respectively.

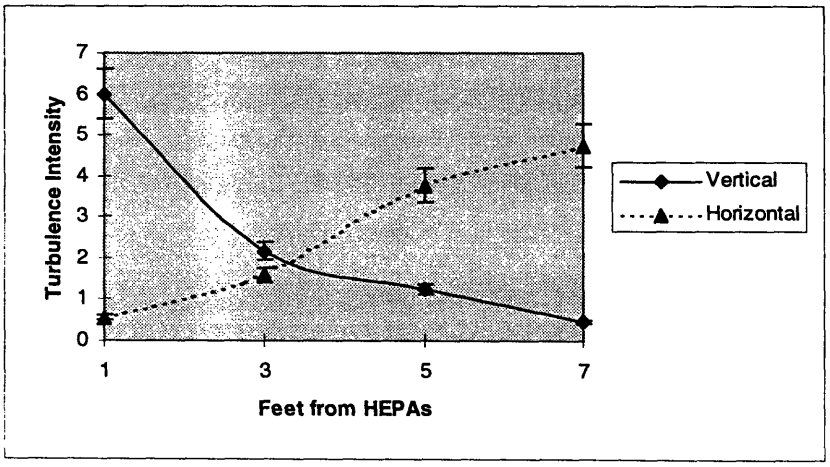

Figure 5.3(a)-Turbulence Intensities in the 50FPM Center Test Region

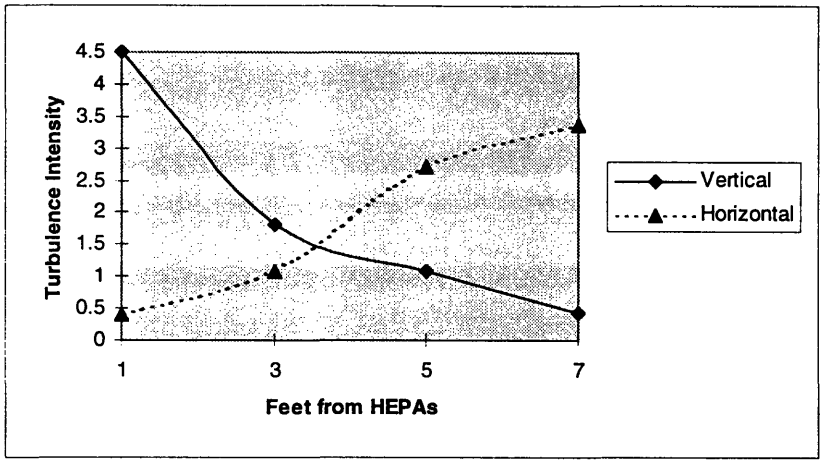

Figure 5.3(b)-Turbulence Intensities in the 70FPM Center Test Region

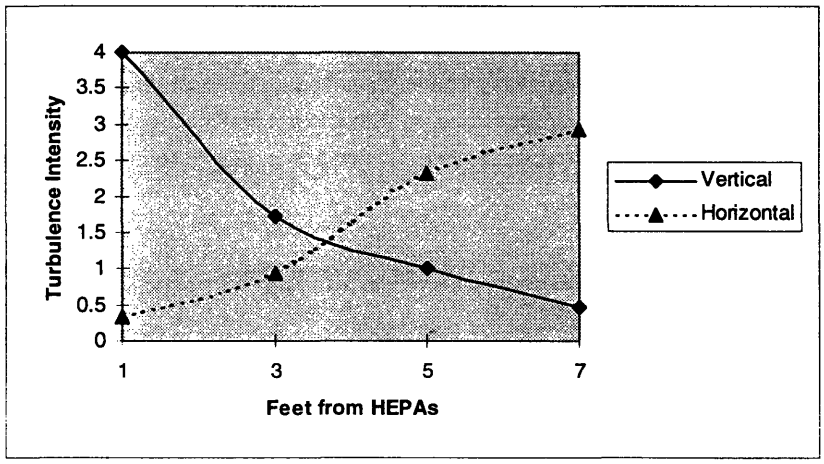

Figure 5.3(c)-Turbulence Intensities in the 90FPM Center Test Region

The 50 FPM vertical turbulence intensity curve indicates a rapidly decreasing intensity towards the floor. Although the velocity reading 3 feet from the HEPA(Level B) indicates

a loss of 43% in turbulence intensity, the reading 7 feet from the HEPA(Level D) demonstrates an 87% loss. In the case of 70 FPM, the velocity reading 3 feet from the HEPA(Level B) indicates a loss of 41%, and an 85% loss by the reading 7 feet from the HEPA(Level D). Similarly, in the 90FPM case, the velocity reading 3 feet from the HEPA(Level B) depicts a 39% loss in turbulence intensity, and an 82% loss by the reading 7 feet from the HEPA(Level D). The respective losses in vertical turbulence intensity are summarized in Table 5.1:

Velocity	1 Ft from HEPA (Level A)	3 Ft from HEPA (level B)	5 Ft from HEPA (Level C)	7 Ft from HEPA (Level D)
50 FPM	0%	44%	78%	87%
70 FPM	0%	41%	77%	85%
90 FPM	0%	39%	74%	82%

Table 5.1- Losses in Vertical Turbulence Intensity in center regions

These observations have profound results because with a significant decrease in turbulence intensity, initial modeling of homogeneous turbulent flow may become inapplicable. Previous research from Batchelor indicates that when a turbulent flow loses more than 50% of its initial turbulence intensity within the length of the flow path, it may or may not retain similar flow patterns[22]. With this guideline, the research may safely assume homogeneous turbulent flow exists slightly below level B, approximately 4 feet from the HEPAs, but not below.

As seen in the complementing horizontal turbulence intensities, the vertical turbulence intensity is not "lost", but rather transferred into crossflow [23]velocities. The

horizontal intensities of the 50FPM velocity illustrate a 59% increase 5 feet from the HEPA(Level C). Similarly the 70FPM and 90FPM velocities demonstrate a 61% and 62% increase, respectively. Table 5.2 illustrates the data below.

Velocity	1 Ft from HEPA (Level A)	3 Ft from HEPA (level B)	5 Ft from HEPA (Level C)	7 Ft from HEPA (Level D)
50 FPM	0%	11%	59%	74%
70 FPM	0%	9%	61%	71%
90 FPM	0%	8%	62%	70%

Table 5.2-Increases in Horizontal Turbulence Intensity in center regions

Unfortunately, the experimental apparatus could not capture all of the turbulence intensity data in the two dimensional plane. As a result, the losses of vertical turbulence intensities do not correspond exactly with the increases in the horizontal intensities. However, the gathered data still indicates a departure from vertical homogeneous turbulent flow towards an increasing horizontal crossflow near the floor. Since return grilles provide negative pressures, much of the neighboring air is drawn away from the vertical flow and transferred into crossflow. In this manner, return grilles not directly underneath an air stream may create a secondary flow which alters the mean velocities as well as causes the measured losses/increases in turbulence intensities.

The turbulence intensity plots of air streams directly above floor grilles illustrate a more unidirectional path. Figures 5.4(a)-(c) indicate the downflow velocity retains a large part of its initial turbulence intensity as far away as 5 feet from the HEPA

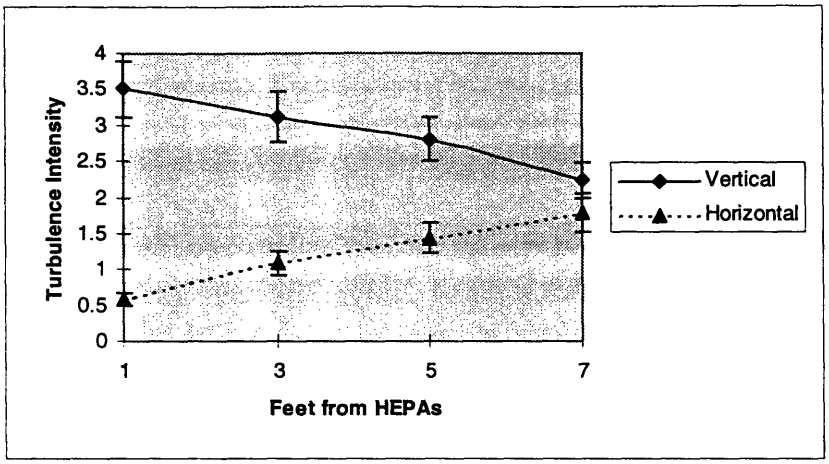

Figure 5.4(a)-Turbulence Intensities in the 50FPM floor grille region

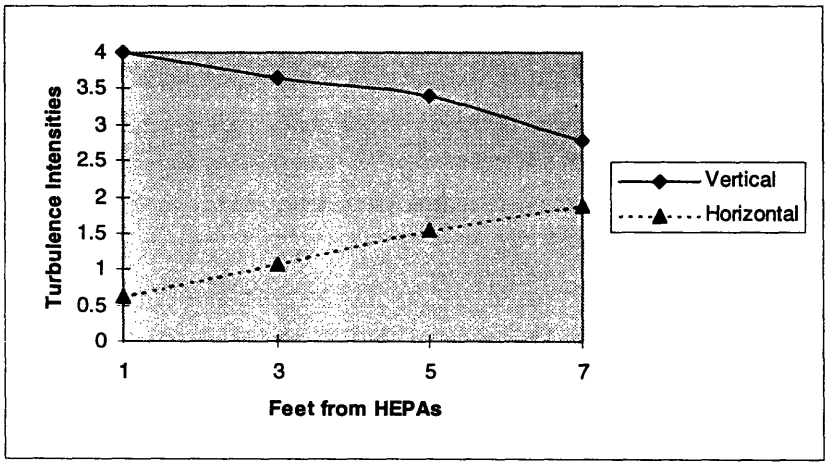

Figure 5.4(b)- Turbulence Intensities in the 70 FPM floor grille region

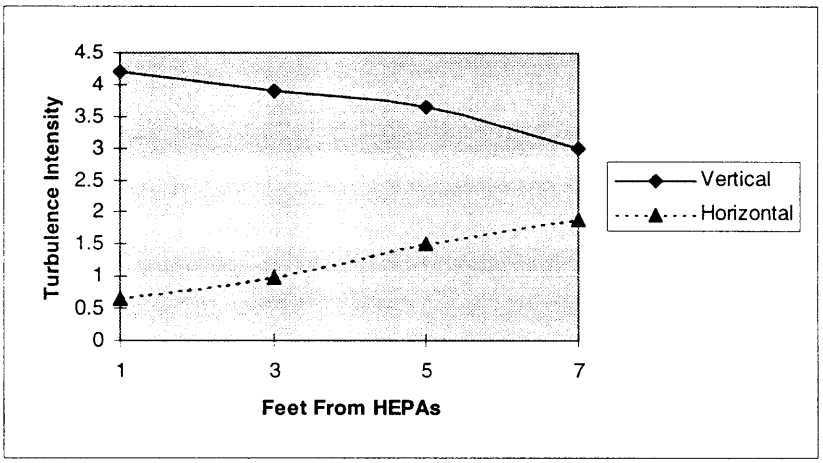

Figure 5.4(c)- Turbulence Intensities in the 90FPM floor grille region

These results reflect homogeneous turbulence to a level slightly below Level C, approximately 6 feet from the HEPAs. These results, however, are anticipated because VLF has previously illustrated that perforated floor grilles directly beneath an airflow aid in maintaining the flow's unidirectionality. However, by averaging the instantaneous anemometer readings to obtain experimental mean velocities, this research has nonetheless confirmed that there is little difference between the unidirectionality of a 90 FPM profile and a 50 FPM profile in regions near floor grilles. Tables 5.3 and 5.4 illustrate the data.

Velocity	1 Ft from HEPA (Level A)	3 Ft from HEPA (level B)	5 Ft from HEPA (Level C)	7 Ft from HEPA (Level D)
50 FPM	0%	10%	21%	30%
70 FPM	0%	8%	17%	27%
90 FPM	0%	5%	14%	25%

Table 5.3- Losses in Vertical Mean Velocities in floor grille regions

Velocity	1 Ft from HEPA (Level A)	3 Ft from HEPA (level B)	5 Ft from HEPA (Level C)	7 Ft from HEPA (Level D)
50 FPM	0%	13%	25%	40%
70 FPM	0%	9%	21%	36%
90 FPM	0%	7%	17%	31%

Table 5.4- Increases in Horizontal Mean Velocities in floor grille regions

Figures 5.5(a)-(c) indicate the turbulence intensities near side wall returns have a different pattern. The vertical turbulence intensity decreases steadily until shortly after Level B, 3 ft from the HEPAs, where the effects of crossflow cause a sudden increase in turbulence intensity.

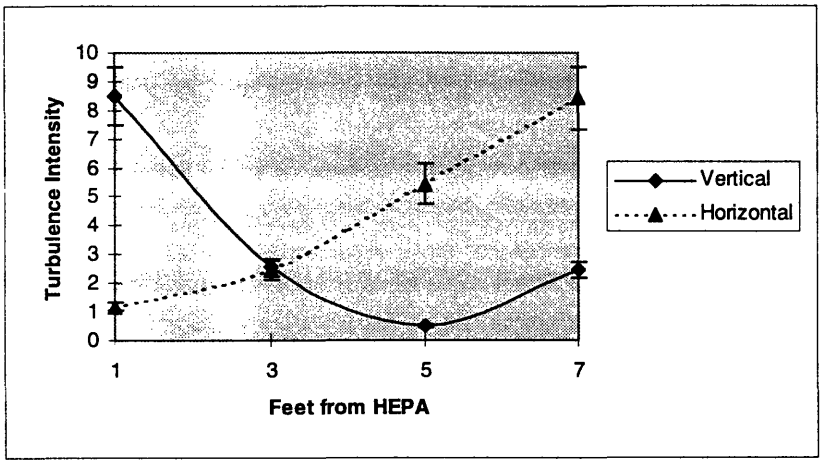

Figure 5.5(a)-Turbulence intensities in the 50 FPM side wall region

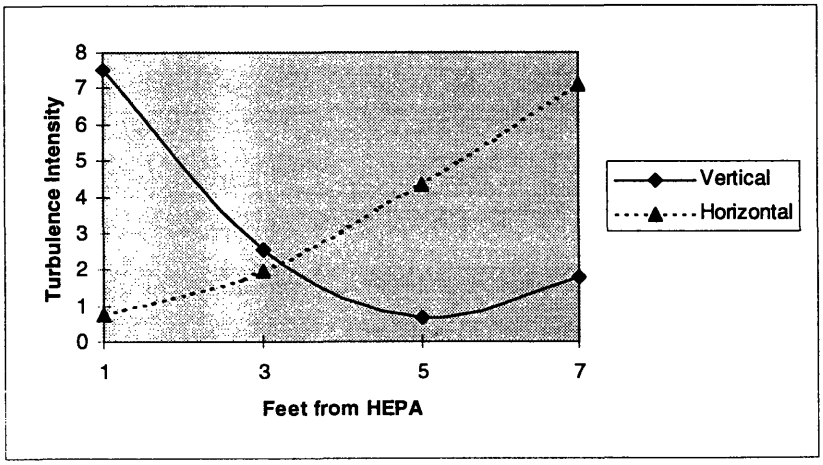

Figure 5.5(b)- Turbulence Intensities in the 70FPM side wall region

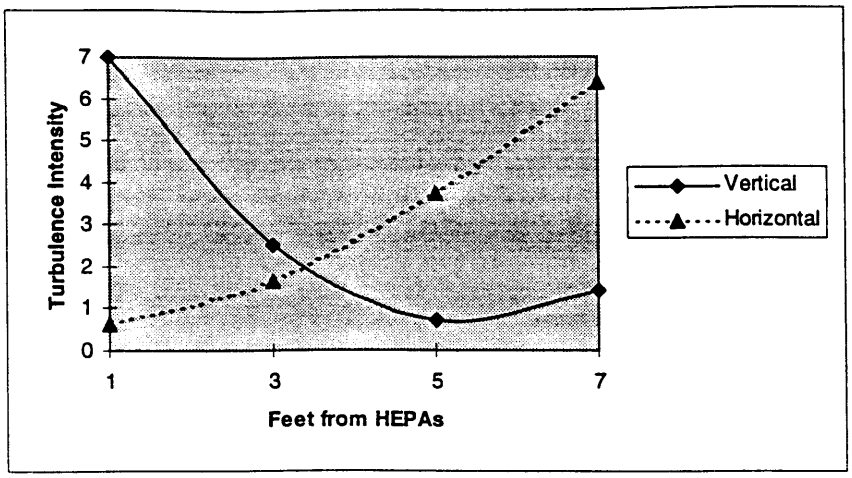

Figure 5.5(c)- Turbulence Intensities in the 90FPM side wall region

This phenomenon is a function of the dimensions and location of the sidewall grille. The grille measures 1 foot by 1 foot and is mounted 1 foot above the clean room floor. Because particles will often impact the grille mesh at odd angles, they may be pushed back into an eddy several times before being extracted through the grille. Particles re-displaced into eddies may be pulled towards the floor by gravitational effects where they can swirl indefinitely before extracted through floor grilles. This generates larger crossflow velocities and increases turbulence intensity as illustrated in Table 5.5.

Velocity	1 Ft from HEPA (Level A)	3 Ft from HEPA (level B)	5 Ft from HEPA (Level C)	7 Ft from HEPA (Level D)
50 FPM	0%	29%	64%	97%
70 FPM	0%	26%	58%	93%
90 FPM	0%	25%	53%	92%

Table 5.5- Increases in Horizontal Turbulence Intensity in sidewall regions

Initially, the sidewall results seem misleading. How can a flow lose turbulence intensity and then regain it so quickly without additional energy? The answer to this question lies in the increase of horizontal mean velocities, turbulence intensity and in the location of the probes. Because sidewall grilles extract flows utilizing so large a surface area, the horizontal mean velocity increases so quickly that close to the sidewall there is often reversed flow during air extraction. Unfortunately, the anemometers used during these experiments are incapable of measuring reverse flows and consequently, data seen past level C, 5 feet from the HEPAs, is inconclusive.

5.3- Particle Deposition Rates

Characterizing turbulent velocity profiles permits the analysis of their effects on particle deposition. In the three test regions of each velocity, the following particle deposition rates were observed:

Air Velocity (Feet Per Minute)	Particles on Wafers (Center)	Particles on Wafers (Floor Grille)	Particles on Wafers (Wall Grille)
50 FPM	45	54	120
70 FPM	51	238	407
90 FPM	56	316	546

Table 5.6- Particle Deposition Data

The data implies that clean rooms operating at higher air velocities will sustain increased deposition rates. This phenomenon may be attributed to air blast issues associated with higher velocities. When a particle is introduced into a clean room in the form of a jet, the flow pattern of that particle is heavily dependent on the velocity of the pre-existing air stream. A particle is immediately displaced by the existing air velocity and is moved towards the floor by gravity and the flow's inertia. Further, the flow's turbulence may displace the particle into an eddy. In this manner the particle is moved further and further away from the perimeter of its source until it is exhausted through a return grille. Flows with higher air velocities generate both greater inertial effects on particles, and stronger eddy currents. Eddy currents are undesirable because they may circulate particles towards the floor at faster speeds or embed them in stagnant zones more readily. Particles caught in flows of high turbulence intensity are also more likely to depose onto the surfaces directly beneath them. Conversely, lower air velocities generate smaller inertial effects, which displace particles towards the floor at slower speeds, and may or may not generate eddies.

The phenomenon of displacing particles through flow inertia effects is commonly called air blasting. Fan units literally blast large flow rates of air into a clean room anticipating the large air volume will flush out particles more readily. As the data implies, air blasting does flush particles into a strong vertical path, however, in many cases this may not be the best method of particulate removal. For instance, if particles are generated above clean room products, air blasting will only cause these particles to depose onto the surface directly beneath them, i.e. the product. Although clean rooms

have evolved at an incredible pace, they continue to rely upon human operators to carry wafers to different work stations or handle products in different apparatus. Since humans generate tremendous amounts of particles at any given instant, there are many operator generated particles hovering above product wafers. Air blasting will only force these particles directly onto the wafer surface. Thus, although particle concentration may be lower at 90 FPM, the deposition of particles is the greater issue.

The data of Table 5.6 demonstrates operational clean rooms with 50FPM or 70 FPM velocities will exhibit reduced particle deposition in production areas; but will the flow pattern determine where the remaining particles travel? To answer this question one must study the specific airflow patterns in the room. Typically, particles are either extracted through return grilles or remain caught in turbulent eddies near the floor. Hence, wherever particle deposition is a major concern, it is often useful to employ flow visualization techniques to make particular particle paths known. As a result, fluorescent particles were used in these experiments to provide such an analysis. Using a black light and enclosing curtains, the path flow of the injected particles was visually observed. The different particle paths for the center, sidewall and floor grille locations in each of the 50FPM, 70FPM, and 90FPM air velocities are shown in Figures 5.6(a)-(l):

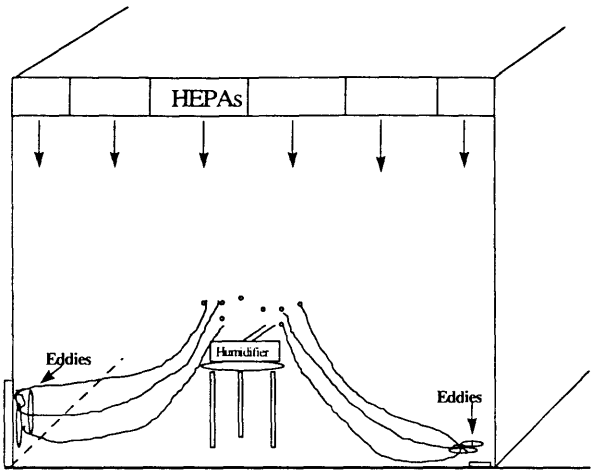

Figure 5.6(a) 50FPM - Center Region

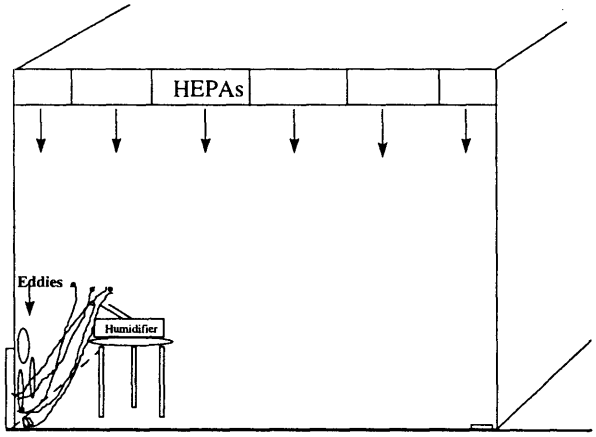

Figure 5.6(b) 50FPM - Sidewall Region

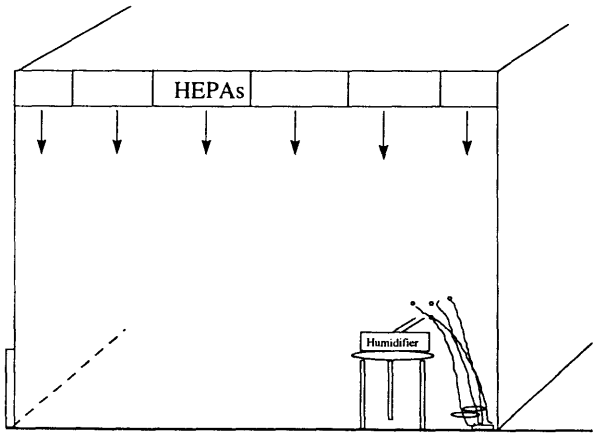

Figure 5.6(c) 50FPM - Floor Grille Region

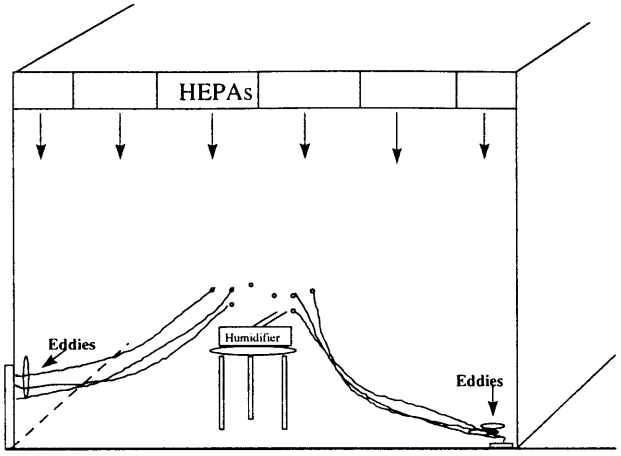

Figure 5.6(d) 70FPM - Center Region

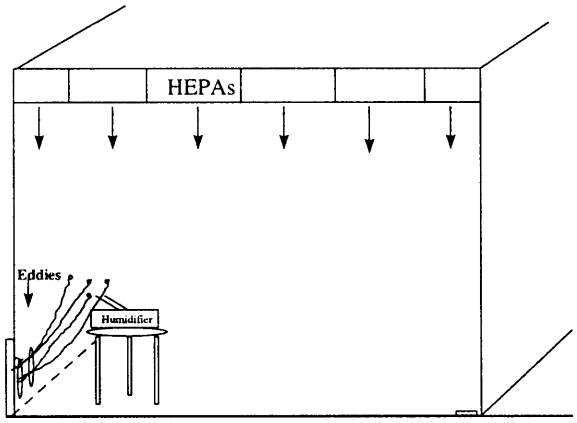

Figure 5.6(e) 70FPM - Sidewall Region

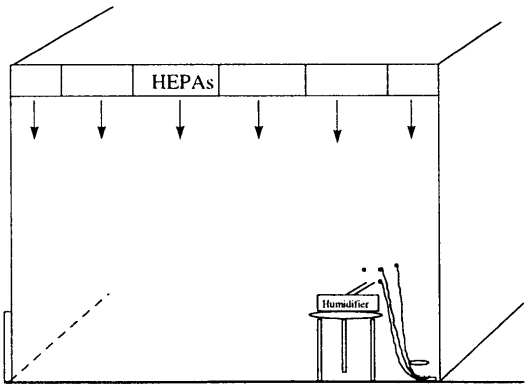

Figure 5.6(c) 70FPM -Floor Grille Region

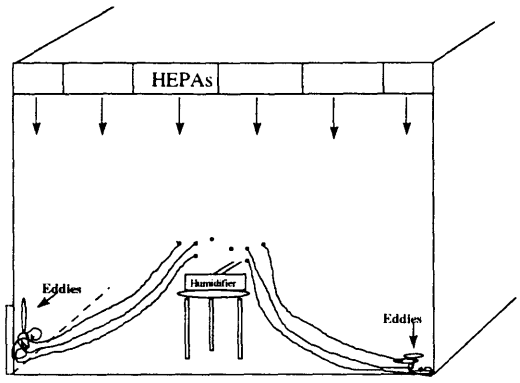

Figure 5.6(g) 90FPM - Center Region

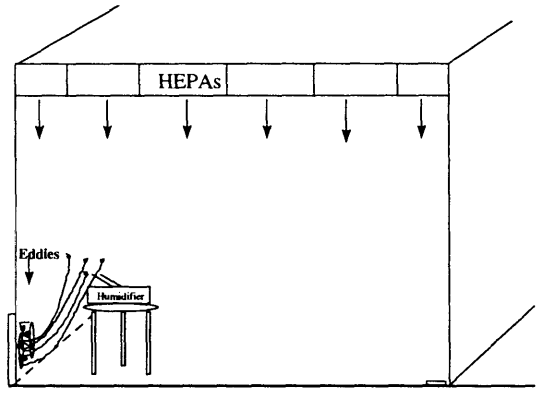

Figure 5.6(h) 90FPM - Sidewall Region

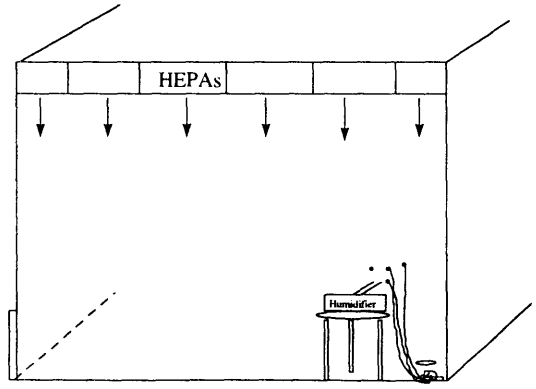

Figure 5.6(I) - Floor Grille Region

Using a stop watch, particle retention times were measured from the time particles were injected until the time when all particles were exhausted. At 50 FPM, the remaining particles remained somewhat stagnant near the floor grilles. Their periodic circulation in the air implied they were caught in slow moving eddies with relatively long dissipation rates. At 70FPM and 90 FPM the remaining particles were also observed to gather near floor grilles. However, although their motion implied particles were also embedded in some type of eddy, these eddies exhibited shorter dissipation rates. In the center region of the 50FPM velocity, particles circulated in eddies for 110 seconds before dissipating out of the area versus 65 seconds and 45 seconds for the 70 FPM and 90 FPM cases respectively. Table 5.7 denotes the experimental results.

Velocity	Center	Floor Return	Sidewall Return
50 FPM	110 seconds	52 seconds	68 seconds
70 FPM	65 seconds	31 seconds	75 seconds
90 FPM	45 seconds	20 seconds	70 seconds

Table 5.7- Timed eddy dissipation rates in all test regions

In each case, particles exited the most quickly in the region near floor grilles. Once again, this may be attributed to the enhanced unidirectionality created by the floor grilles themselves. Smaller increases in horizontal turbulence intensities combined with lower losses in vertical intensities create a vertical, streamline path which purges out particles more readily.

5.4 Analysis of Velocity Profiles

Utilizing the data gathered with hot wire anemometers in the test grid, velocity profiles were generated from two dimensional velocity vectors. Figures 5.6, 5.7 and 5.8 depict velocity profiles where solid lines represent actual measurements and dashed lines represent symmetry. The profiles exhibited similar flow patterns and similar effects on particles. The differences were in the actual number of particles counted near the exit grilles and in crossflow velocities. It is interesting to note that although the different velocity patterns yield different turbulent ranges and particle counts, all three indicate a "Tee-Pee" effect towards the center of the room. "Tee-pee" is the commonly used term for an air stagnant zone created when vertical moving air separates to exhaust through different return grilles. This research measured the sizes of each tee pee by moving the probe rake to over 25 locations within each air stagnant zone. The tee pee symbol was placed in regions where anemometer readings were on the order of the natural convection velocity or less. The Tee-pees measured throughout these experiments may be attributed to the lack of a raised floor configuration which forces the air to travel to the nearest return grille. Although proper balancing and certification will insure air does not travel towards one side over another, these precautions will not prevent flow separation near the floor.

Studying Figure 5.7, an increase in crossflow shortly after level B dissipates air unidirectionality in the 50 FPM case.

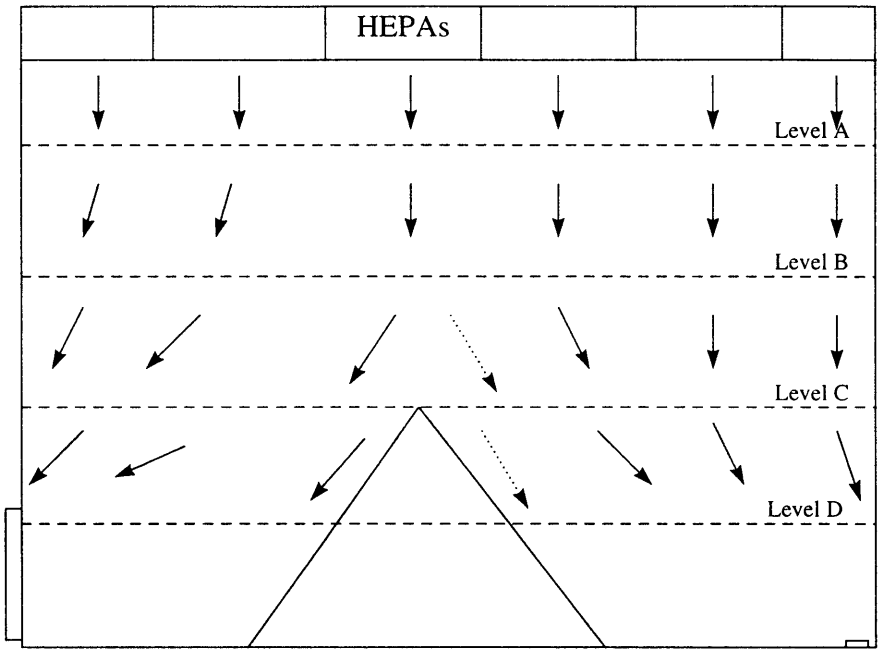

Figure 5.7- 50FPM Velocity Profile

In this instance, the tee-pee is observed to form at level C, as increasing crossflows carry particles towards return grilles with minimal direct vertical deposition.

Observing Figure 5.8, one notices a smaller departure from unidirectionality than in the previous 50FPM case. This may be attributed to the flow's slower decay in vertical turbulent intensity and smaller increase in crossflow. As a result, the 70FPM profile maintains unidirectional air streams more readily, but its increased velocity additionally results in higher particle concentrations near side wall and floor returns. In this instance, the tee-pee effect is observed to begin at a slightly lower elevation than level C, because of its better unidirectionality.

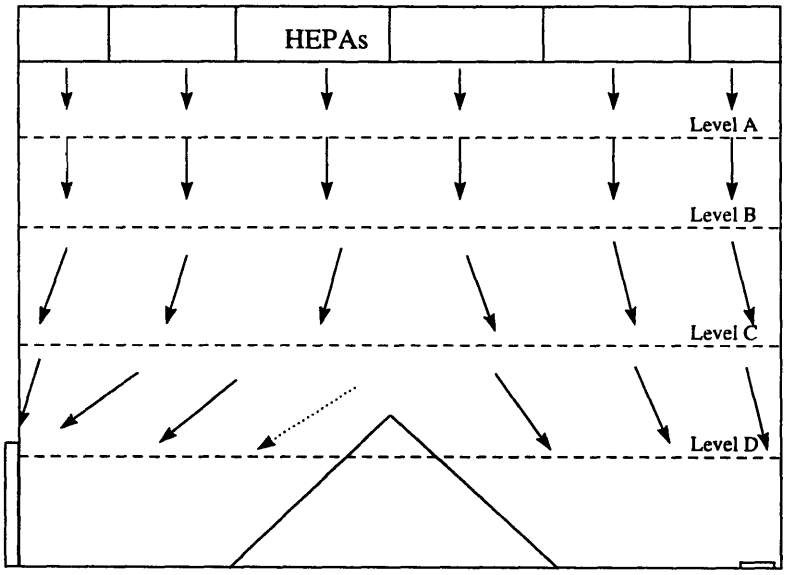

Figure 5.8 - 70 FPM Velocity Profile

Figure 5.9 illustrates a significant increase in the unidirectionality of an air stream in the 90FPM case profile. Here, a smaller increase in crossflow does not disturb the vertical flow pattern from the HEPA until an elevation close to level C. As a result, particles remain in the streamline pattern and are flushed out more readily through floor grilles. However, an increased velocity means an increase in particle deposition rate as observing the Tee-pee effect at the lowest level, close to level D, implies particles are flushed vertically towards product surfaces.

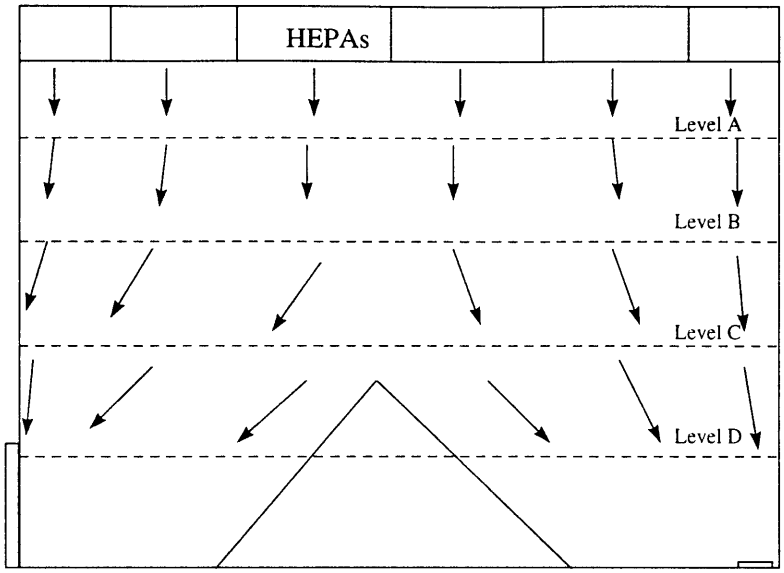

Figure 5.9 - 90FPM Velocity Profile

5.5 Conclusions

In conclusion, the results of these experiments illustrate two phenomenon; the correlation between increased air velocities and particle deposition rates, and the relationship between turbulence patterns at room elevations. Velocity profiles and turbulence intensity graphs have illustrated the limits of air unidirectionality. Throughout the 50FPM, 70FPM and 90FPM experiments, unidirectionality was consistently demonstrated through levels midpath to exhaust grilles. Each level displayed a slightly different turbulent flow path as levels A and B maintained homogeneous turbulence but levels C and D did not. Secondly, particle measurements indicated that increased air velocities produce slightly more unidirectional airflow, but produce higher particle deposition rates. In areas where human operators must handle wafers or products directly, the benefits of increased air unidirectionality are outweighed by the increased probability of particle deposition and subsequent product failure. As mentioned earlier,

each facility must be analyzed individually. However, this research has demonstrated that a typical clean room facility may operate at 50FPM or 70FPM to decrease deposition rates and simultaneously remain in its current class level.

Analyzing solely the energy savings in the air handling fan units, a velocity reduction will substantially reduce the size and wear on clean room fans. By utilizing the fan laws, when a sample 1,000 ft^2 clean room facility has its velocity reduced from 90 FPM to 70 FPM, there is an 83% reduction in Brake Horse Power(BHP) and a 68% decrease in static pressure.

Fan 1:	Fan 2:
90 FPM	70 FPM
4.5 in w.g.	1.4" in w.g.
10.2BHP	1.74BHP

Fan Laws:

$$\frac{RPM_2}{RPM_1} = \frac{Q_1}{Q_2} \qquad \text{(23)}$$

$$\frac{P_2}{P_1} = \left(\frac{RPM_2}{RPM_1}\right)^2 \qquad \text{(24)}$$

$$\frac{FP_2}{FP_1} = \left(\frac{RPM_2}{RPM_1}\right)^3 \qquad \text{(25)}$$

Where Q= Airflow(CFM)
P= Pressure(in w.g.)
FP = Fan Power(BHP)

Additionally, by reducing clean room air velocities to 70FPM from 90FPM, the electrical power required for each fan, would be reduced to almost half its original consumption.

The proceeding fan equation indicates a 20% velocity reduction coupled with a 30% reduction in pressure, results in a 48% power reduction:

$$P_f = \dot{m}\frac{\Delta P}{\rho} \qquad \text{(26)}$$

Where P_f = Fan Power
m = Mass flow rate
ΔP = Change in Pressure
ρ = Fluid density

An average 1000ft^2 facility operating with 90FPM air velocities consumes $14,000 of fan electricity annually. Implementing a 20% velocity reduction to 70FPM would save a facility of this size roughly $7,000 a year. Similarly, implementing a velocity reduction in a typical 64,000ft^2 facility would result in an annual savings of $448,000.

Furthermore, applying the before mentioned annual cost of $25 per CFM of air exhaust, a small facility of 1000ft^2 will save approximately $2,500 a year:

$$\frac{20Ft}{Min} \times 1{,}000\,ft^2 \times \frac{\$25\,yearly}{1\,{}^{ft^3}\!/_{\min}} = \$500{,}000\,yearly$$

@ 0.5% yearly exhaust ---- > $2,500 a year

This same algorithm yields a cost reduction of $320,000 a year for a typical 64,000ft^2 clean room facility.

Hence, although clean room history has traditionally demanded 90FPM air velocities, the increased costs, consumption of energy and of natural resources, in the larger facilities make this requirement unrealistic and costly. Reducing to 70FPM or 50FPM velocities will often save hundreds of thousands of dollars a year in operating costs, reduce particle deposition and simultaneously retain class levels. In conclusion,

the results of this research warrant a paradigm shift to lower air velocities in operating and future clean room facilities. Unique specifications for each clean room facility, will prevent engineering design from antiquated models, significantly reduce operating costs, and perhaps most importantly, limit the superfluous usage of energy and natural resources from local communities.

5.6- Uncertainty Issues

5.6.1- Rake

Although the rake was positioned and constructed as stable as possible, due to its height and slender body, it inevitably maintains a relative finite motion with respect to ground. The swaying motion may cause additional crossflow measurements or even falsely increase downflow measurements. However, these swaying motions occur at extremely low frequencies. Because of the chosen sampling rate, this research generates graphs from 0 to 100 kHz frequencies which facilitates the extraction of this lower frequency data.

5.6.2 Probes

One key element of this research was the manufacture of hot wire anemometer probes. Although the casings used were TSI models, due to the fragile nature of the wires, the hot wires repeatedly disattached. To avoid high replacement fees from the manufacturer, this research opted for spot welding methods to repair broken anemometers. The disadvantage of this method is that each probe wire varies a finite amount in length based on human error or craftsmanship. Spatial resolution is limited

by the length of the wire and different length hot wire anemometers will lead to a variation of heat transfer and temperature across the wire.

Another accuracy issue may be raised with the electrical circuit. As mentioned earlier, each design incorporates two potentiometers. These variable resistors provide large benefits of enabling adjustable bias voltages, however, their strong disadvantage is how easy it is to adjust this voltage unintentionally or after every use. Their resistances are altered through screw switches which may easily turn on their own due to movement or vibration. To compensate for this, potentiometer resistances were calibrated with a voltmeter before every experiment to insure accurate values.

The Metrabyte Easyest LX software was chosen because of its ability to provide a large frequency response to the data. Hot-Wire Anemometers have a high frequency response and turbulence data would not have been possible with a sampling frequency less than 10kHz. The frequency response data was gathered at a 100kHz sampling frequency which permitted the acquisition of a large percentage of ranging fluctuations. However, such a large sampling frequency became a limitation as the computer was unable to store such large amounts of data for each test point. As a result, in order to retain data values for each probe, the experiments were limited to using only a fraction of a second after steady state had been reached. Although the time scale was short, each probe data file contains a minimum of 64000 points. From calibration tests, the computer software and hot wire data, the experimental apparatus has an uncertainty of 7%.

5.6.3- Facilities

One crucial aspect of these tests is the ability to accurately reduce air velocities in the operating clean room; this was accomplished through a reduction in fan velocity. However, the particular TRL facility has several fans feeding a combination of areas. Hence, a fan reduction does not correspond to a one to one uniform velocity reduction in the experimental space. To compensate for this issue, a hand held anemometer was used to determine the velocity just downstream of each HEPA filter in the test grid. With this test, experiments did not proceed until the velocity across each HEPA was uniform and equal in magnitude. Although usage of hand held self calibrating instruments during experiments is often frowned upon by researchers, in this instance it was most certainly necessary and was virtually insignificant in the data acquisition itself.

5.7- Further Study

Although these tests have illustrated the strong dependency on particle deposition to air velocities, they could not model the effects of personnel movement in the clean room. Various studies have proven there are significant wakes behind moving persons in clean rooms which would certainly effect the velocity profile and its purging capacity. To make these test more comprehensive, further study incorporating clean room operator movement in each velocity profile and measurement of the recovery time for unidirectional airflow would be optimal.

Additionally, this research would have benefited greatly from the use of computational fluid dynamics to model the experimental area. Since CFD may provide over 100 times the resolution of these experiments, this data would have greatly enhanced the reliability of the CFD predictions had they been done concurrently.

Bibliography

1. Austin, P.R. Design and Operation of Clean Rooms. Troy, Michigan: Business News Publishing Company, 1970. pp 1-9

2. Batchelor, H.K. The Theory of Homogeneous Turbulence. London: Cambridge Press 1952 pp 5-14

3. Bowling, A., Davis, C. "Managing Contamination during advanced Wafer Processing," Solid State Technology February 1994 pp 45-47

4. Bradshaw, P. Turbulence and its Measurement New York: Spring Verlag 1978 pp 128-131

5. Bradshaw, P. Turbulence New York: Springer Verlag 1978

6. Busnaina, A. "Modeling of Airflow and Particle Transport in Cleanrooms," Proceedings, 10th ICCS 1990 International Symposium on Contamination Control pp 276-280

7. Coleman, L.A. "Contamination Control Market to double by the Year 2000," CleanRooms Magazine April 1996

8. Cooper, M.G. "Air Treatment Design for Clean Rooms," Building Design Partnership 1993

9. Dunn, P.N. "The unexpected benefits of ISO 9000," Solid State Technology March 1994 pp 55-57

10. English, S. "Handling/Delivery systems Keep Vigorous Pace with Semiconductor Growth," CleanRooms magazine, March 1996 pp 20-28

11. George, W.K., Buether, P.D., Shabbier, A. "Polynomial Calibration for Hot-Wires in Thermally varying Flows," 1987 Fluids Symposium on Thermal Anemometry pp 36-47

12. Hattori, T. "Contamination Control: Problems and Prospects," Solid State Technology July 1990 pp 45-51

13. Heyns, M. "Ultra-Clean or 'just clean enough' Technology?," Solid State Technology December 1994 p 23

14. Hinze, O.J. Turublence. New York: McGraw-Hill 1975

15. Hunt, Phillips, Williams Turbulent and Stochastic Processes: Kolmogorov's Ideas 50 Years on. London: Royal Society 1991

16. Jorgenson, F. "Measurement of Low Turbulence Flows using Hot Wire Anemometry," Dantec Technologies Technical Paper 34590-2 pp 3-17

17. Jorgenson, F. "Signal Processing and Hot Wire Anemometry," Dantec Technologies Technical Paper 34560-1 pp 2-5

18. Kozicki, M., Hoening, S., Robinson, P. Cleanrooms. Van Nostrand Reinhold, New York. 1991 pp 118-124

19. Leinhard, III. Measurements in Mechanical Engineering. Cambridge, Mass.: MIT Press 1989

20. Leslie, D.C. Developments in theTheory of Turbulence. Oxford: Claredon Press 1983

21. Lieberman, A. "Airborne Particles in Cleanrooms," Particle Measuring Systems Technical Paper 3456-82 April 1989

22. Marvell,G. "Minienvironment Air Flow Design," Solid Sate Technology, August 1993 pp 47-51

23. Mei, R. "Dispersion of Particles with Non Linear Drag and Restoring Force in Turbulent Flows," 1993 ASME Gas Particle Flows pp 47-65

24. Murakami, S., Shinsuke, K. "3-D Numerical Simulation of Air Flow in Clean rooms by neams of a 2 Equation Model," ASHRAE 1987 Annual Meeting, Nashville, TN.

25. "Semiconductors: When the Chips are Down," The Economist, March 23, 1996 pp 19-21

26. Soules, W. "Airflow Management," CleanRooms Conference East 1996 Proceedings

27. Stainback S., Nagabushara, N. "Review of Hot-Wire Anemometry Techniques and Range of their Applications," 1993 ASME Symposium on Thermal Anemometry pp 3-34

28. Stock, D.E. "Particle dispersion in Flowing Gases," Journal of Fluids Engineering, March 1996 pp 21-32

29. Tan-Athichat, J., Nagib, H.M., Loehrke, R.I. "Interaction of Free Stream Turbulence with Screens and Grids: A Balance Between Turbulent Scales," Journal of Fluid Mechanics, 114:501-528

30. Townsend, A.A. The Structure of Turbulent Flow. Cambride England: Cambridge University Press 1976

31. WIS Automatic Wafer Inspection System Operating Instructions. Aeronca Electronics Inc. 1984 pp 2-7

[1] "Semiconductors: When the Chips are Down," The Economist, March 23, 1996 pp 19-21
[2] Austin, P.R. Design and Operation of Clean Rooms. Troy, Michigan: Business News Publishing Company, 1970. pp 1-9
[3] Kozicki, M., Hoening, S., Robinson, P. Cleanrooms. New York: Van Nostrand Reinhold, 1991 pp 118-124
[4] Austin, P.R. Design and Operation of Clean Rooms. Troy, Michigan: Business News Publishing Company, 1970. pp 1-9
[5] Coleman, L.A. "Contamination Control Market to double by the Year 2000," CleanRooms Magazine, April 1996
[6] Kozicki, M., Hoening, S., Robinson, P. Cleanrooms. New York: Van Nostrand Reinhold 1991 pp 118-124
[7] Batchelor, H.K. TheTheory of Homogeneous Turbulence. London: Cambridge Press 1952 pp 5-14
[8] Bradshaw, P. Turbulence and its Measurement New York: Spring Verlag 1978 pp 128-131
[9] Batchelor, H.K. TheTheory of Homogeneous Turbulence. London: Cambridge Press 1952 pp 45-61
[10] J. Tan-Athicaht, H.M., Nagib, R.I. "Interaction of Free Stream Turbulence with Screens and Grids: A balance between Turbulent Scales," Journal of Fluid Mechanics, 114 pp 501-528
[11] Soules, W. "Airflow Management," CleanRooms Conference East 1996 Proceedings
[12] English, S. "Handling/Delivery systems Keep Vigorous Pace with Semiconductor Growth," CleanRooms magazine, March 1996 pp 20-28

[13] Lieberman, A. "Airborne Particles in Cleanrooms," Particle Measuring Systems Technical Paper 3456-82 April 1989
[14] Mei, R. "Dispersion of Particles with Non Linear Drag and Restoring Force in Turbulent Flows," 1993 ASME Gas Particle Flows pp 47-65
[15] Busnaina, A. "Modeling of Airflow and Particle Transport in Cleanrooms," Proceedings, 10th ICCS 1990 International Symposium on Contamination Control pp 276-280
[16] English, S. "Handling/Delivery systems Keep Vigorous Pace with Semiconductor Growth," CleanRooms magazine, March 1996 pp 20-28
[17] Jorgenson, F. "Measurement of Low Turbulence Flows using Hot Wire Anemometry" Dantec Technologies Technical Paper 34590-2 pp 3-17
[18] Leinhard, III. Measurements in Mechanical Engineering. Cambridge, Mass: MIT Press 1989
[19] Stainback S., Nagabushara, N. "Review of Hot-Wire Anemometry Techniques and Range of their Applications," 1993 ASME Symposium on Thermal Anemometry pp 3-34
[20] Jorgenson, F. "Signal Processing and Hot Wire Anemometry" Dantec Technologies Technical Paper 3456-7 pp 2-5
[21] WIS Automatic Wafer Inspection System Operating Instructions. Aeronca Electronics Inc. 1984 pp 2-7
[22] Batchelor, H.K. TheTheory of Homogeneous Turbulence. London: Cambridge Press 1952 pp 4-21